agriculture

MDPI

Article

Pollen Development and Stainability in *Vicia faba* L. and *Lupinus angustifolius* L.

Wiktor Skrzypkowski [1], Renata Galek [2], Adela Adamus [1] and Agnieszka Kiełkowska [1,*]

[1] Faculty of Biotechnology and Horticulture, University of Agriculture in Krakow, Al. Mickiewicza 21, 31-120 Krakow, Poland; wiktor.skrzypkowski@student.urk.edu.pl (W.S.); a.adamus@urk.edu.pl (A.A.)
[2] Department of Plant Genetics, Breeding and Seed Production, Wroclaw University of Environmental and Life Sciences, Grunwaldzki 24a, 50-363 Wrocław, Poland; renata.galek@upwr.edu.pl
* Correspondence: a.kielkowska@urk.edu.pl

Abstract: Commercially, leguminous crops (*Fabaceae*) are the second most important group of cultivated plants, just after grasses (*Poaceae*). This study focuses on the analysis of pollen development and stainability in two species belonging to the Fabaceae family: *Vicia faba* L. and *Lupinus angustifolius* L. Morphological analysis of the anthers at various stages of flower development allowed us to trace the processes of microsporogenesis and microgametogenesis. Nine different cell staining protocols with diverse mechanisms of action, including acetocarmine, Alexander's dye, aniline blue in lactophenol, Calcein AM, FDA, MTT, TTC, Lugol's iodine, and aceto-orcein, were tested for their suitability in assessing the viability of microspores as well as pollen grains in both species. Among the applied dyes, four allowed for the discrimination between viable and nonviable microspores in *V. faba*, and six dyes allowed for this in *L. angustifolius*. For mature pollen grains, all dyes enabled differentiation between viable and nonviable cells in both species. The highest viability indications for *V. faba* microspores were obtained with acetocarmine (94.6%), while for mature pollen, aniline blue in lactophenol, MTT, and aceto-orcein yielded the highest viability indications (90.8–96.3%). In *L. angustifolius*, the highest percentages of viable microspores (64.9–66.5%) were obtained with the acetocarmine, aniline blue in lactophenol, and TTC dyes. For mature pollen, the highest viability indications (83.4%–92.9%) were obtained with acetocarmine, aniline blue in lactophenol, Lugol's iodine, and aceto-orcein. The viability of *V. faba* pollen grains in an in vitro germination test showed that the highest pollen germination (61.3%) was observed on the BK medium (rich in minerals with 10% sucrose). In *L. angustifolius*, the highest pollen germination was observed on the media containing boric acid and 5% sucrose (70.5%) and on the medium containing 10% sucrose only (74.2%).

Keywords: faba bean; lupin; microspore; pollen germination; pollen development; viability

Citation: Skrzypkowski, W.; Galek, R.; Adamus, A.; Kiełkowska, A. Pollen Development and Stainability in *Vicia faba* L. and *Lupinus angustifolius* L. *Agriculture* **2023**, *13*, 2065. https://doi.org/10.3390/agriculture13112065

Academic Editors: Jaime Prohens, Penelope Bebeli and Vasileios Papasotiropoulos

Received: 3 October 2023
Revised: 24 October 2023
Accepted: 25 October 2023
Published: 27 October 2023

1. Introduction

Leguminous crops, belonging to the *Fabaceae* family (also known as legumes), are plants of among the highest commercial importance worldwide, and rank among the top crops in terms of global production, reaching approximately 190 million tons in 2021 [1–3]. Legumes are important in human nutrition due to the high protein content in their seeds. Grain legumes such as soybeans (*Glycine max*), chickpeas (*Cicer arietinum*), pigeon peas (*Cajanus cajan* L.), cowpeas (*Vigna unguiculata* L.), beans (*Phaseolus vulgaris* L.), field peas (*Pisum sativum* L.), lentils (*Lens esculenta Moench*), faba beans (*Vicia faba* L.), and grasspeas (*Lathyrus sativus* L.) account for 27% of world crop production and provide 33% of the dietary protein consumed by humans [4,5]. Seeds of legumes are also rich in carbohydrates and dietary fiber, and to a lesser extent, lipids, bioactive peptides, and polyphenols, and for this reason, legumes are also widely used as fodder crops. The most important forage legumes are alfalfa (Medicago sativa), clover (*Trifolium* sp.), vetch (*V. sativa*), and lupin (*Lupinus* sp.) [5–7]. Legumes are also important in natural ecosystems and agriculture due to their nitrogen fixation ability in symbiosis with nodule-forming bacteria [8].

The high commercial and economic significance of leguminous crops drives the need for the development of advanced breeding methods focused on creative breeding and improvement of cultivated varieties (yield, resistance, chemical composition). Biotechnological methods have emerged as a branch of modern plant breeding, allowing for the acceleration of the breeding process, which is crucial in the context of global environmental changes and the reduction in cultivation areas [9]. One such method is the production of homozygous lines through in vitro manipulation in the process of haploidization of plant materials. Obtained through this process, doubled haploid (DH) plants are highly significant in plant breeding, as they considerably shorten the breeding process [10,11]. Some haploidization methods rely on manipulations of male gametophyte cells. These methods include androgenesis (in isolated anther cultures and isolated microspore cultures) and induction of parthenogenesis through distant pollination or pollination by artificially inactivated pollen [11–14]. The above-mentioned techniques, as well as conventional plant breeding processes based on controlled pollination, require precise determination of cell viability (both microspores and mature pollen), necessitating the optimization of procedures and the selection of appropriate methods for assessment.

Vicia faba (also known as the broad bean, fava bean, or horse bean) and *Lupinus angustifolius* (also known as narrow-leaved lupin or blue lupin) are plants for which little progress has been made in the development of haploidization methods, including those based on the induction of male gametophyte cell development [15–18]. The first step for successful in vitro manipulation of isolated microspores during haploidization is an efficient monitoring system to determine their viability [19]. Similarly, pollen viability estimation is crucial during controlled pollination, after inactivation procedures, or in the verification of the degree of male sterility in plants [20,21]. Therefore, the optimization of methods aiming at determination of the viability of microspores and pollen grains in plants is needed. In *L. angustifolius* and in *V. faba*, such knowledge would be valuable in terms of gaining a better understanding of flowering biology and assessing the physiological conditions of both microspores (i.e., for haploidization) and mature pollen (i.e., for breeding). To the best of our knowledge, for both species, there are no comprehensive studies on the analysis of pollen development beginning from pollen mother cells to mature pollen. Moreover, information on the assessment of microspore viability and comparative studies on pollen viability testing in either *L. angustifolius* or *V. faba* are lacking.

Pollen viability estimation in plants is based on two approaches: chemical staining and germination testing. Chemical staining is a common technique in the assessment of pollen viability. This technique is based on colorimetric reactions of dye with cytoplasm proteins (acetocarmine, Alexander's dye, benzidine), nuclei (acetocarmine,), cell walls (Alexander's dye), vacuoles, or secretory cells (neutral red), or with cellular components such as starch (Lugol's dye), callose (aniline blue), lipids (Sudan stains), or nucleic acids (acetocarmine, 4′,6-diamidino-2-phenylindole (DAPI)) [22–25]. Chemical staining techniques also determine cell enzymatic activity; i.e., tetrazolium salt (MTT) detects dehydrogenase activity [26], and fluorescein diacetate (FDA) and calcein are used for detection of esterase activity within plant cells [27,28]. It should be noted that differences have been reported in optimal staining techniques, and chemical staining methods are not universal and often require adaptation to the specific plant species [25,27,29,30]. In contrast, germination assays determine the actual germination ability of mature pollen (not applicable for microspores) under suitable conditions. The germination is performed under laboratory conditions and is greatly influenced by several factors, such as the genotype of the evaluated accession, the germination medium composition, temperature, and humidity [31,32].

The aim of this study was to trace the processes of microgametogenesis and microsporogenesis leading to the development of functional male gametophyte cells in *V. faba* and *L. angustifolius*, and to find an optimal method for determining the viability of microspores and pollen grains in both species, for which similar investigations have not been conducted so far. In pursuit of the stated aims, cytohistological analyses of microtome sections of the floral buds of both species at different stages of development were performed

and selected methods for assessing the viability of microspores and pollen grains were employed. This involved the application of specific dyes known for their utility in evaluating cell viability, which operate through diverse mechanisms. Additionally, a set of pollen germination media with varying compositions was tested to assess their effectiveness in determining the viability of mature pollen grains in the species under investigation.

2. Materials and Methods

2.1. Plant Material and Growth Conditions

Two cultivars (Bartek and Rambos) of *Vicia faba* and two cultivars (Karo and Regent) of *Lupinus angustifolius* were investigated. Donor plants of both species were obtained from seeds. Seeds were commercial samples. Seeds of *V. faba* were sown into 12 L pots filled with compost soil/peat mixture (1:1). Donor plants of *V. faba* were grown in growth chamber under controlled conditions of 16/8 h photoperiod supplied using sodium lamps (Lucalox LU600W/PSL, GE Lighting, Budapest, Hungary). The plants were kept in temperatures of 18–20 °C during the day and 15–16 °C during the night and were optimally irrigated and fertilized. *L. angustifolius* plants were grown from April to July and August to October in open-air experimental plot at Agriculture University in Kraków (Poland), located in Prusy near Kraków (50°07′00.6″ N, 20°05′13.6″ E). The temperatures during cultivation were on average 18–25 °C during the day, and 15–18 °C during the night. Field-grown plants were watered as needed and fertilized. Plants of both species started to flower approximately two months after seed sowing. After being collected from the donor plants, flower buds and flowers were kept in a vessel with a moistened paper towel to avoid dehydration of plant material. Plant materials were analyzed on the day of collection.

2.2. Anatomical Examination of Anthers

For anatomical examination, flower buds of both species and each cultivar in different developmental stages (based on different bud sizes, approximately 2–8 mm and ≥9 mm) were collected and fixed in Carnoy's fluid (3 volumes absolute ethanol and 1 volume glacial acetic acid). Fixation was performed for at least 48 h in a fridge at a temperature of 6 ± 1 °C. After fixation, samples were subjected to dehydration in graded ethanol series (70%, 80%, 90% (*v*/*v*), kept 15 min in each) and then left overnight in absolute ethanol. On the next day, buds were submerged and embedded in Technovit® 7100-embedding resin (Kulzer, Hanau, Germany) according to protocol provided by manufacturer. Blocks of polymerized resin containing plant samples were cross-sectioned into 4 µm slices using Leica RM2145 rotary microtome (Leica Microsystems, Wetzlar, Germany) equipped with carbide blade (Leica TC-65, KAWA.SKA, Zalesie Górne, Poland). Cross-sections were then stained with 1% (*w*/*v*) toluidine blue (Sigma-Aldrich, Darmstadt, Germany), and mounted with Entellan™ (Merck, Darmstadt, Germany). Microscopic examination of anthers and pollen development was performed using Axio Imager M2 (Carl Zeiss, Göttingen, Germany) microscope in bright field mode.

2.3. 4′,6-Diamidino-2-phenylindole (DAPI) Staining

DAPI staining was performed prior to rapid assessment of pollen developmental stage in collected buds and flowers. Various lengths (4–8 mm and ≥9 mm) of *V. faba* and *L. angustifolius* flower buds were collected and then anthers were subsequently isolated. Dissected anthers were macerated on a glass slide in a drop of DAPI solution (2.5 µg mL^{-1} DAPI, 7.7 mM Tris-HCl, 10 mM spermine tetrahydrochloride, 10 mM NaCl, 2.2% (*v*/*v*) hexylene glycol, and 0.25% (*v*/*v*) Triton™ X-100) and mixed with glycerine in equal proportion. The DAPI solution was kept in a dark glass bottle and stored at 4 °C. After maceration, the remains of the anther tissue were gently removed and the slides were covered with a coverslip. All the slides were analyzed under Axio Imager M2 (Carl Zeiss, Göttingen, Germany) microscope equipped with fluorescence mode with the appropriate filter set for DAPI (Zeiss filter set 02; λ_{Ex} = 365 nm, λ_{Em} > 420 nm). In this experiment, a minimum of 300 cells per slide was counted (with one slide per bud/flower and 3–5 buds/flowers for each explant size and for each cultivar).

2.4. Cytological Staining of Microspores and Pollen

Flower buds and flowers of both species and studied cultivars were collected over morning hours and kept in a vessel with a moistened paper towel. For microspore and pollen viability assessment, various staining methods were employed. The slide preparation procedure was the same for all dyes and consisted of the isolation of anthers from flower buds of proper lengths (established based on DAPI analysis) for microspores and opened flowers for mature pollen analysis. Then, excised anthers were macerated in a drop of the dye. After removing the remaining anther tissue, the slides were covered with a coverslip. Slides were analyzed after 10 min incubation or after 24 h (depending on staining protocol) under Axio Imager M2 (Carl Zeiss, Göttingen, Germany) microscope in bright field mode or under Leica Dmi8 (Leica Microsystems, Wetzlar, Germany) microscope in fluorescence mode (for visualization of Calcein AM and fluorescein diacetate) at 150× or 300× magnification.

For each stain, a minimum number of 100 cells per slide was counted (with one slide per bud/flower and 4–6 buds/flowers for each cultivar). For cells stained with acetocarmine, Alexander's dye, aniline blue in lactophenol, Lugol's iodine, 2,5-diphenyl tetrazolium bromide (MTT) staining, 2,3,5-triphenyl tetrazolium chloride (TTC) staining, and aceto-orcein, viability was expressed as the percentage of viable pollen. For cells stained with fluorescent dyes (Calcein AM and FDA), the percentage of viable cells was estimated as the proportion of cells emitting fluorescence in relation to all observed cells.

2.4.1. Acetocarmine Staining

To determine viability of microspores and pollen, 2% (*w*/*v*) solution of acetocarmine (Sigma-Aldrich, Poznań, Poland) containing 10 g of carmine in mixture of 225 mL glacial acetic acid and 275 mL distilled water was employed. To prepare solution, carmine powder was first dissolved in acetic acid, then boiled in flask for 30 min, cooled, and filtered through filter paper (medium-quality type 289, Ahlstrom Germany GmbH, Bärenstein, Germany). The stain was kept in dark glass bottles at room temperature (RT). Slides were observed after 10 min incubation at RT in the dark. Acetocarmine stains viable cells pink to red, while nonviable cells are transparent.

2.4.2. Aceto-Orcein Staining

Working solution of aceto-orcein consisted of 1 g of orcein (Sigma-Aldrich, Poznań, Poland), 22.50 mL glacial acetic acid, and 27.50 mL distilled water. This solution was prepared by pouring boiling acetic acid over orcein powder. Then, the solution was cooled and filled with distilled water and filtered through filter paper (medium-quality type 289, Ahlstrom Germany GmbH, Bärenstein, Germany). The solution was stored in dark glass bottles at RT. Stained slides were observed after 10 min incubation at RT in the dark. Viable cells stained dark pink, and nonviable cells were colorless.

2.4.3. Alexander's Staining

The Alexander's staining test is based on differential staining of cytoplasm and cell walls. Dye was prepared by mixing 10 mL of 95% (*v*/*v*) ethanol, 10 mg malachite green, 50 mL distilled water, 25 mL glycerol, 5 g phenol, 5 g chloral hydrate, 50 mg acid fuchsin, 5 mg orange G, and 2 mL glacial acetic acid [33]. The stain was kept in dark glass bottles at RT. Slides were observed after 10 min incubation at RT in the dark. Alexander's dye stains viable cells pink to dark purple. In nonviable cells, the cell interiors remain transparent, while cell walls stain green/blue.

2.4.4. Aniline Blue in Lactophenol Staining

In aniline blue in lactophenol staining test (Lactophenol Cotton Blue), ready-to-use reagent (Sigma-Aldrich, Poznań, Poland, 61335) containing 100 mL of aqueous solution (50 mg aniline blue, 25 g phenol, 25 g L(+)-lactic acid and 50 g glycerol) was employed. The stain was kept in dark glass bottles at RT. After preparation, slides were kept in the

dark at RT for 24 h and then observed. Viable cells stained blue, while nonviable cells were colorless.

2.4.5. Calcein Acetoxymethyl (Calcein AM) Staining

Calcein AM (Calbiochem, Merck, Warsaw, Poland) was made up as a stock solution in dimethyl sulfoxide (DMSO) at 1 mg × mL^{-1}. Stock solution was stored at 4 °C in aliquots. The working solution was made fresh before every use by diluting 1 µL of stock solution in 1 mL of liquid medium used as solvent. The medium consisted of micro- and macronutrients and vitamins according to Gamborg et al. [34] supplemented with 10 mg × dm^{-3} ascorbic acid, 2 mg × dm^{-3} glycine, 250 mg × dm^{-3} casein hydrolysate, 10 mg × dm^{-3} reduced glutathione, 30 g × dm^{-3} sucrose, and 90 g × dm^{-3} maltose. Slides were incubated in the dark at RT for 10 min. Viability of cells was then analyzed using fluorescent microscopy (λ_{Ex} = 495 nm, λ_{Em} = 515 nm). Calcein is a membrane-permeable dye. After entering the cell, intracellular esterases cleave acetoxymethyl ester group, yielding fluorescent calcein. Under fluorescent microscopy, viable cells emit yellow-green fluorescence, while nonviable cells have no fluorescence [35].

2.4.6. Fluorescein Diacetate (FDA) Staining

FDA (Sigma-Aldrich, Poznań, Poland) was prepared as a 0.5% (*w*/*v*) acetone stock solution. Stock solution was stored at 4 °C in aliquots. To prepare a working solution, 15 µL of stock solution was taken and diluted in 0.985 µL of liquid medium used as solvent. The medium used here was the same used for the calcein preparations (see Section 2.4.5.). Then, 50 µL of prepared working solution was diluted in 4 mL of liquid medium. The working solution was made freshly before use. The slides were incubated in the dark at RT for 10 min. Viability of cells was then analyzed using fluorescent microscopy (λ_{Ex} = 485 nm, λ_{Em} = 515 nm). FDA is a membrane-permeable fatty acid ester. Inside living cells, FDA is hydrolyzed by esterases into fluorescent fluorescein. Under fluorescent microscopy, viable cells emit yellow-green fluorescence, while nonviable cells are nonfluorescent [36].

2.4.7. Lugol's Iodine Staining

Ready-to-use reagent of Lugol's iodine solution (COEL, Krakow, Poland) containing 10 mg iodine and 20 mg potassium iodide in 1 g of water solution was used in this protocol. The solution was stored at RT. For staining, samples were put in a drop of Lugol's iodine solution and analyzed immediately. Lugol's iodine detects the presence of starch in the cell's cytoplasm, and viable cells stain dark brown to black, while nonviable cells are colored yellow to bright brown.

2.4.8. 2,5-Diphenyl Tetrazolium Bromide (MTT) Staining

For the cell viability analyses, 1% (*w*/*v*) solution of MTT was employed. Working solution consisted of 1 g of MTT (Sigma-Aldrich, Poznań, Poland) dissolved in 100 mL water–sucrose solution. Water–sucrose solution was prepared by dissolving 5 g sucrose in 100 mL distilled water. The stain was kept in dark glass bottles in a fridge at 6 °C. Slides with stained samples were kept in the dark at RT for 24 h and then observed. The dark pink to dark purple color of cells signaled dehydrogenase activity while the colorlessness of cells showed lack of activity of these enzymes; therefore, pink- to purple-colored cells were considered as viable and colorless cells as nonviable.

2.4.9. 2,3,5-Triphenyl Tetrazolium Chloride (TTC) Staining

For the cell viability analyses, 1% (*w*/*v*) solution of TTC was employed. Working solution was produced by dissolving 1 g of TTC (Sigma-Aldrich, Poznań, Poland) in water–sucrose solution. Water–sucrose solution was prepared by dissolving 12 g of sucrose in 20 mL distilled water. The stain was kept in dark glass bottles in a fridge at a temperature of 6 °C. Similar to MTT staining protocol, slides with stained cells were kept in the dark at RT for 24 h before being observed. The pink- to red-colored cells signaling the activ-

ity of dehydrogenases were considered as viable, while colorless cells were considered as nonviable.

2.5. In Vitro Pollen Germination

For pollen germination test, flowers were collected from the same plants that were used for cytological staining. Analysis was performed on flowers during anthesis containing mature pollen. Pollen germination testswere initiated just after harvesting the flowers. The assessment of pollen germinability was undertaken on the following media: (1) 5% (*w*/*v*) sucrose–water solution; (2) 10% (*w*/*v*) sucrose–water solution; (3) BK medium [37] containing 720 mg dm^{-3} $Ca(NO_3)_2 \times 4\,H_2O$, 200 mg × dm^{-3} $MgSO_4 \times 7\,H_2O$, 200 mg × dm^{-3} KNO_3, 20 mg × dm^{-3} H_3BO_3 and supplemented with sucrose in concentration 10% (*w*/*v*); (4) medium according to Gaaliche et al. [38] containing 5 mg × dm^{-3} H_3BO_3 and supplemented with sucrose in concentration of 5% (*w*/*v*) (marked as 'G medium' in this paper). Each of four different germinating media was solidified with agar (Plant Propagation Lab-Agar, Biocorp, Warsaw, Poland) in concentration of 1% (*w*/*v*). For germination test, a drop of germinating medium was applied on the surface of a microscope slide using glass rod and left approximately 10 min for solidification. Then, pollen was gently distributed on the surface of germinating medium. Slides were then transferred into a humid chamber (Petri dish Ø 150 mm, with a moistened filter paper on the bottom) and incubated for 24 h in the dark at a temperature of 26 ± 1 °C. After incubation, slides were analyzed under Axio Imager M2 (Carl Zeiss, Göttingen, Germany) microscope using phase contrast technique. Pollen grains with clearly distinguishable pollen tubes exceeding the diameter of the pollen grain were classified as germinated, while pollen grains with no pollen tubes were classified as non-germinated.

In this experiment, a minimum of 300 pollen grains on each medium per single cultivar was counted (with one slide per flower and 3 flowers for each cultivar).

2.6. Statistical Analysis

Mean values and standard errors of the means (SEMs) were calculated for each parameter. The overall effect of treatments was assessed using two-way analysis of variance (ANOVA) and Tukey's honestly significant difference (HSD) test at $p \leq 0.05$. Statistical analyses were performed using software R version 4.2.1 (R Core Team, Vienna, Austria, 2022). Experiments on microspores and pollen viability and germination were carried out in three repetitions.

3. Results

3.1. Anatomical Examination of Anthers and Tracking of Pollen Development

3.1.1. *Vicia faba*

In floral buds of 2–3 mm, anthers were approximately 0.5 mm (Figure 1A) and contained pollen mother cells (PMCs) (Figure 1B). PMCs were characterized by their irregular, slightly spherical shape and were surrounded by a thick layer of callose. The nuclei in the PMCs were located in the centers of the cells or were shifted to their peripheral part. The distinct tapetum layer was clearly delineated and consisted of elongated cells and clearly defined large cell nuclei (Figure 1B, asterisk). In buds of 5 mm, anthers became yellowish and were nearly 1 mm (Figure 1C). The anthers contained tetrads (Figure 1D). Tetrads are the cells at the last stage of microsporogenesis following meiotic division of the pollen mother cell. The tetrads of *V. faba* were surrounded by callose, and under microscopic view, three cells could be clearly observed, while the fourth was located beneath. The tapetum layer was also clearly visible, and the cells with centrally located large nuclei took on a more cubic form than in anthers containing PMCs (Figure 1D, asterisk). In 6–7 mm buds, anthers were approximately 1–1.5 mm (Figure 1E). These anthers contained uninucleate microspores (Figure 1F). The microspores were separated from one another and were spherical or slightly elongated and contained large, centrally located nuclei. In 6.5–7 mm flower buds, anthers contained cells with polarized nuclei. The tapetum layer started to degenerate and individual cells started to be seen as separated (asterisk in Figure 1F). In

flower buds larger than 8 mm, the anthers exceeded 1.5 mm (Figure 1G). The majority of the cells observed in such anthers had an elongated shape and exhibited two round nuclei. The tapetum layer was completely degenerated and was not present under microscopic view. Furthermore, in the microscopic image, the anther wall did not display such distinct layering as was observed in younger anthers. Endothecium cells at that stage were clearly distinguishable, and they were larger compared with the epidermal cells and thickened by cellulosic deposits, stained light blue with toluidine blue ('en' in Figure 1H).

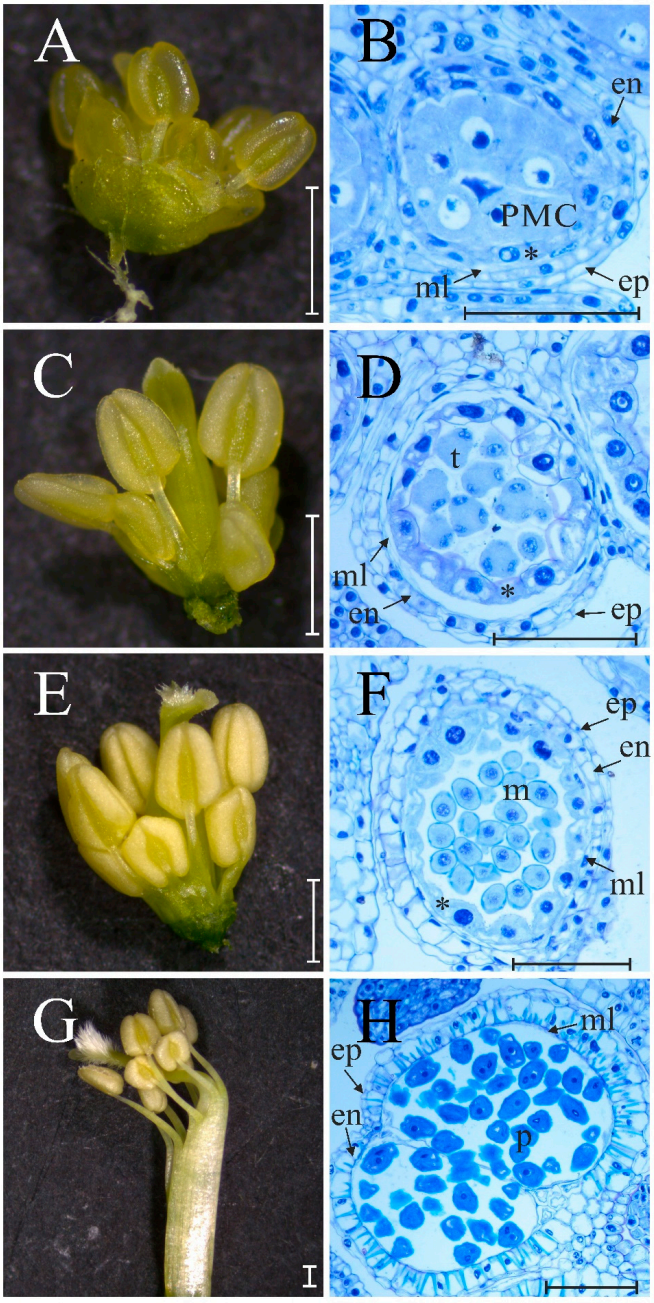

Figure 1. Morphology (the **left** panel) and cross-sections (the **right** panel) of *Vicia faba* anthers in different developmental stages: (**A**,**B**)—anthers containing pollen mother cells (PMCs); (**C**,**D**)—anthers containing tetrads; (**E**,**F**)—anthers with microspores at uninucleate stage; (**G**,**H**)—anthers with pollen grains. Figure legend: PMC—pollen mother cell, t—tetrads, m—microspores at uninucleate stage, p—pollen, ep—epidermis, en—endothecium, ml—middle layer; asterisks indicate tapetum. Bars in left panel = 1 mm, bars in right panel = 100 μm.

3.1.2. *Lupinus angustifolius*

In approximately 2 mm flower buds of *L. angustifolius*, the anthers were near 0.5 mm in length and were bright green (Figure 2A). Anthers at that stage contained PMCs exclusively (Figure 2B). These cells were large and irregular in shape, with a distinct cell nucleus located in the central part of the cell. The PMCs exhibited intensive blue staining, in both the cytoplasm and nucleus, with toluidine blue. Additionally, in such anthers, the different layers of the anther wall (epidermis, middle layer, endothecium, and tapetum) could be clearly distinguished (Figure 2B). In flower buds measuring 3–4.5 mm (Figure 2C), anthers had a length of approximately 1 mm and became bright orange. Such anthers contained tetrads, which were surrounded by a brightly stained callose layer (Figure 2D). In cross-section, distinct layers of anther walls could be clearly observed. At this stage, the tapetum exhibited a deep blue stain when treated with toluidine blue. In 5–6 mm (Figure 2E) flower buds, anthers had a length of approximately 1–1.5 mm and possessed a thick cell wall divided into three layers. The tapetum, however, was not as distinct as in the tetrad stage, and was observed as a slightly bluish layer irregularly present beneath the middle layer. In such anthers, uninucleate microspores were mainly found (Figure 2F). They appeared as large cells with a spherical or near-spherical shape, with a centrally located cell nucleus. In anthers isolated from buds closer to 6–6.5 mm, the microspores contained polarized nuclei, shifted to a cell pool. In flower buds longer than 7 mm (Figure 2G), predominantly two-nucleate pollen grains (Figure 2H) were commonly found. The cells comprising the final stage of microgametogenesis within the anther displayed irregular shapes, ranging from triangular to elongated, with dark-stained cell nuclei.. However, the two cell nuclei were not always clearly contrasted in the microscopic image. The anther wall in such anthers exhibited differentiated layers in cross-section, while the tapetum was already completely degraded. The endothecium was clearly distinguishable, and its cells were thickened by cellulosic deposits ('en' in Figure 2H).

3.2. Nuclear Stain (DAPI) for Determination of the Stage of Pollen Development

DAPI analysis was performed to determine the relation between floral bud length and pollen developmental stage, and to validate the anatomic observations. This was important for the selection of optimal floral bud length for further analyses. In both species, 4–8 and $\geq$9 mm floral buds and flowers were analyzed, and differences in the percentages of certain pollen developmental stages according to the flower buds' sizes between tested cultivars within the species were found.

3.2.1. *Vicia faba*

The results of the analysis of the stage of pollen development after DAPI staining in *V. faba* are presented in Figure 3A–C and Figure 4. In 4–5 mm 'Bartek' flower buds, tetrads (Figure 3A) were found in prevalence (82.5–97.4%). The 'Rambos' flower buds of 4 mm in size contained tetrads (74.77%), and uninucleate microspores (Figure 3B) were predominant (58.24%) in buds of 5 mm in size. The anthers of 6 mm floral buds contained mainly uninucleate microspores in both cultivars ('Bartek'—100%, 'Rambos'—99.67%); however, in 'Rambos' a small number of tetrads (0.33%) was found as well. In 7 mm floral buds, uninucleate microspores and binucleate cells (Figure 3C) in both cultivars were observed, though in 'Bartek' they were in equal proportions and in 'Rambos' uninucleate microspores were in the majority (80%). In the largest analyzed flower buds (8 and $\geq$9 mm) and opened flowers, only binucleate cells were found in both cultivars.

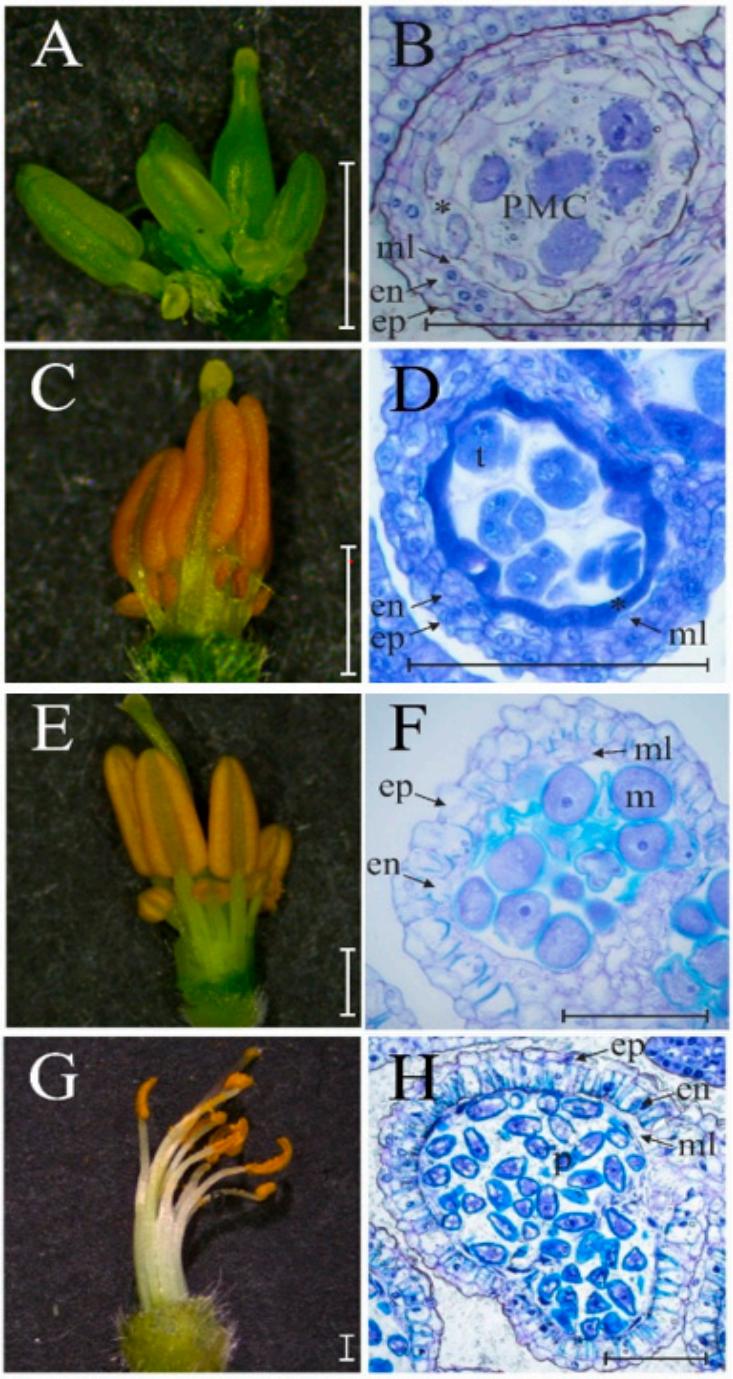

Figure 2. Morphology (the **left** panel) and cross-sections (the **right** panel) of *Lupinus angustifolius* anthers in different developmental stages: (**A**,**B**)—anthers containing pollen mother cells (PMCs); (**C**,**D**)—anthers containing tetrads; (**E**,**F**)—anthers with microspores at uninucleate stage; (**G**,**H**)—anthers with pollen grains. Figure legend: PMC—pollen mother cell, t—tetrads, m—microspores at uninucleate stage, p—pollen, ep—epidermis, en—endothecium, ml—middle layer; asterisks indicate tapetum. Bars in left panel = 1 mm, bars in right panel = 100 μm.

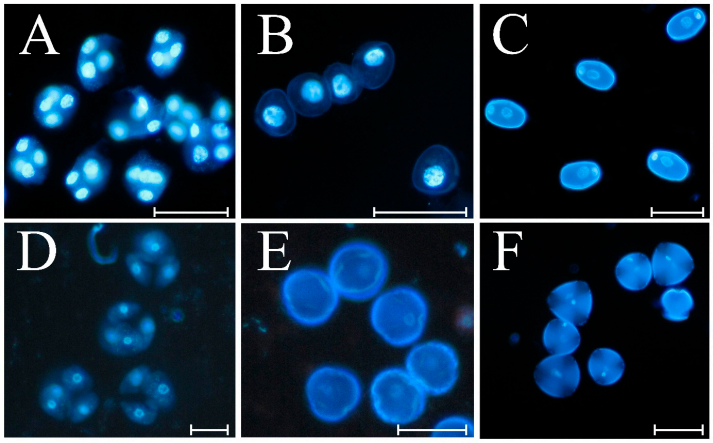

Figure 3. The different developmental stages of microspores and pollen of *Vicia faba* (**upper** panel) and *Lupinus angustifolius* (**lower** panel) after DAPI staining: (**A**,**D**)—tetrads; (**B**,**E**)—uninucleate microspores; (**C**,**F**)—binucleate pollen grains. Bar = 50 µm.

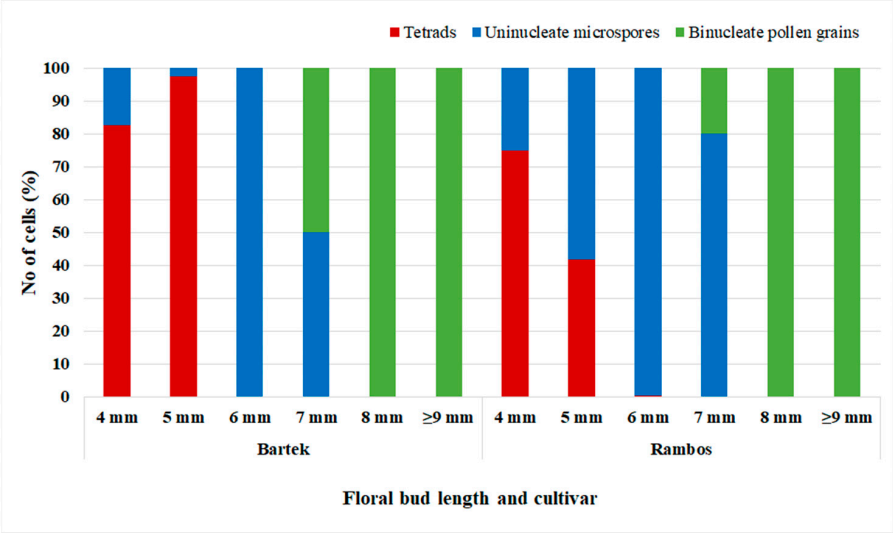

Figure 4. Distribution of developmental stages of pollen depending on flower bud length in *Vicia faba* cultivars Bartek and Rambos.

3.2.2. *Lupinus angustifolius*

The results of the analysis of pollen development after DAPI staining in *L. angustifolius* are presented in Figure 3D–F and Figure 5. In 4 mm 'Karo' floral buds, the presence of tetrads (Figure 3D) was observed sporadically (9.20%). In 4–5 mm floral buds, mainly uninucleate microspores (90.80–100%) were observed in both cultivars. Floral buds of 6 mm contained uninucleate microspores (Figure 3E) and binucleate cells (Figure 3F) in different proportions depending on the cultivar: in 'Karo' the percentage of uninucleate microspores relative to binucleate cells was, respectively, 55.50% to 45.50%, while in 'Regent' it was 91.05% to 8.95%. Similar results were observed in 7 mm buds: in 'Karo' buds there was an 88.87% proportion of uninucleate microspores and 11.13% proportion of binucleate cells, whereas in 'Regent' there was a 79.51% proportion of uninucleate microspores and 20.49% proportion of binucleate cells. In 'Karo' floral buds that were 8 mm in length, binucleate cells were predominant (91.31%), but uninucleate microspores (8.69%) were also observed. In similar 'Regent' buds, only binucleate cells were found. In the largest analyzed (9 mm) flower buds of both *L. angustifolius* cultivars, binucleate pollens were observed exclusively.

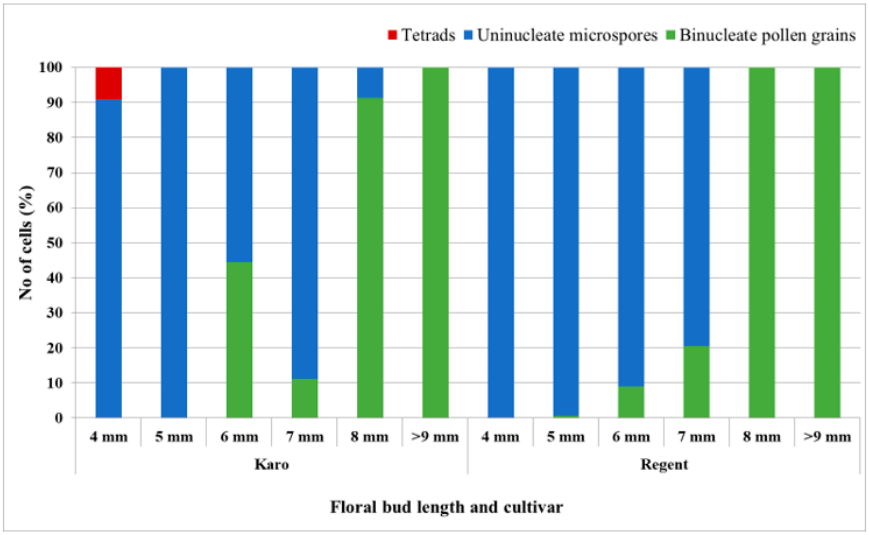

Figure 5. Distribution of developmental stages of pollen depending on flower bud length in *Lupinus angustifolius* cultivars Karo and Regent.

3.3. Cytological Staining of Microspores and Pollen

In total, nine different staining methods for the evaluation of microspore and pollen viability in both tested species were employed. The results are shown separately for each species.

3.3.1. *Vicia faba*

In *V. faba*, only four (acetocarmine, Alexander's dye, FDA, and Calcein AM) out of the nine tested stains allowed for discrimination between viable and nonviable microspores (Figure 6). The analysis of the stainability of *V. faba* cells showed that acetocarmine applied on microspores stained the cytoplasm bright pink, while the nucleus was clearly visible and stained red. Nonviable microspores were transparent (Figure 6A). Alexander's dye stained the cell walls of viable microspores green-blue and the cytoplasm purple-pink; however, the staining was not evenly distributed. In most observed cells, the dye was accumulated within some regions of the cell interior (mostly terminal) and was rarely observable within the whole volume of the cells. Nonviable microspores had light blue or transparent cytoplasm and blue cell walls (Figure 6B). Both fluorescent dyes (Calcein AM and FDA) gave a similar effect and viable microspores emitted yellow-green fluorescence while nonviable microspores had no fluorescence (Figure 6C,D,I,J). In some samples stained with Calcein AM and FDA, the fluorescent signals were very weak, making the observations difficult. The remaining stains, i.e., aniline blue in lactophenol, Lugol's iodine, MTT, TTC, and aceto-orcein, were ineffective and did not allow for discrimination of viable and nonviable microspores of *V. faba*.

The results of cell microspore viability depending on the staining method are presented in Table 1. The average viability of *V. faba* microspores, calculated as the mean from all dyes that discriminated viable and nonviable cells, was 66.21%; however, differences in viability were observed depending on the stain used. The highest microspore viability (94.57%) was detected after the application of acetocarmine, lower (80.05%) after the application of Alexander's dye. The lowest percentage of viable microspores was indicated using dyes detecting esterase activity; Calcein AM showed only 16.28% viable microspores and FDA showed 20.35%, whereas microspore viability indicated using dyes detecting cytoplasmic content (acetocarmine and Alexander's dye) was four- to almost six-fold higher (80.05–94.57%).

Table 1. Viability of *Vicia faba* pollen and microspores determined with different staining methods.

Staining Method	Viability (% ± SEM)	
	Microspores	Pollens
Acetocarmine	94.57 ± 0.79 ^{a}	84.28 ± 1.61 ^{bc}
Alexander's dye	80.05 ± 2.78 ^{b}	82.84 ± 1.74 ^{c}
Aniline blue in lactophenol	-	96.30 ± 0.62 ^{a}
Calcein	16.28 ± 3.12 ^{c}	31.78 ± 2.32 ^{d}
FDA	20.35 ± 1.65 ^{c}	38.81 ± 2.19 ^{d}
Lugol's iodine	-	85.57 ± 1.28 ^{bc}
MTT	-	93.67 ± 0.89 ^{a}
TTC	-	86.38 ± 1.38 ^{bc}
Aceto-orcein	-	90.80 ± 1.26 ^{ab}
Total	66.21 ± 2.43	80.55 ± 0.77

Means in column with the same letters are not significantly different according to Tukey's HSD test ($p \leq 0.05$). The dyes marked with a dash (-) did not allow for discrimination between viable and nonviable cells.

The viability of *V. faba* microspores depending on the cultivar is presented in Figure 7. The results showed no difference in the viability of microspores between the tested *V. faba* cultivars after acetocarmine (90.90–98.20%) and Calcein AM (13.70–19.50%) staining. Using Alexander's method for staining, more viable microspores (90.20%) were detected in 'Rambos' compared with 'Bartek' (72.40%). However, after applying FDA, higher viability (28.0%) was detected among microspores of 'Bartek', compared with 'Rambos' (13.50%).

All nine stains were also used for analysis of the viability of mature pollen. All of them allowed for the discrimination of viable and nonviable pollens of *V. faba* (Figure 6). Pollen grains were stained completely differently using acetocarmine compared with microspores, as all the cytoplasm of the pollens was stained intense red, and the nuclei were barely recognizable within the cells. Nonviable pollens stained pale pink (Figure 6E). Alexander's dye stained the cytoplasm of viable mature pollen an intense purple-pink with distinctively blue cell walls. The nonviable pollen grains contained no cytoplasm; therefore, only the cell walls were stained blue (Figure 6F). Similar to the microspores, the pollen grains stained with fluorescent dyes (Calcein AM and FDA) emitted yellow-green fluorescence if they were viable and had no fluorescence if nonviable (Figure 6G,H,L,M). Both the TCC and MTT dyes detecting dehydrogenase activities stained the interior of the pollens, and these were considered viable. A lack of dehydrogenase activity resulted in a lack of staining of the cytoplasm. TTC stained viable pollen grains deep red, while nonviable grains were transparent (Figure 6K). MTT dye stained viable pollen dark purple to nearly black, while nonviable grains were transparent (Figure 6N). If starch grains in the cells' cytoplasm were detected, Lugol's iodine clearly stained viable pollen grains dark brown to black. If starch was not detected in the cytoplasmic content, the cells were stained bright brown, which provided the distinction between viable and nonviable cells (Figure 6O). Aniline blue in lactophenol is a dye that detects callose in a plant's cell wall. Mature pollen grains of *V. faba* that were stained with this stain were dark blue, and nonviable ones were transparent (Figure 6P). The observations for the TTC, MTT, and aniline blue in lactophenol stains were performed 24 h after preparation of the microscopic slides, which was considered as the most optimal time for the discrimination of viable and nonviable pollen grains. Longer exposure of cells to these stains decreased the effectiveness of the observations due to the blurring of differences between viable and nonviable cells and problems with distinguishing cells from the background (the background became too dark). On the other hand, too short a period of exposure to the mentioned dyes caused the cells to not be properly stained (meaning they were unstained and undercolored). The aceto-orcein detected cytoplasmic content but also visualized clearly the cell nuclei in pollen grains of *V. faba*. Viable grains turned dark pink and elongated nuclei were clearly seen, while nonviable cells were stained pale pink (Figure 6Q).

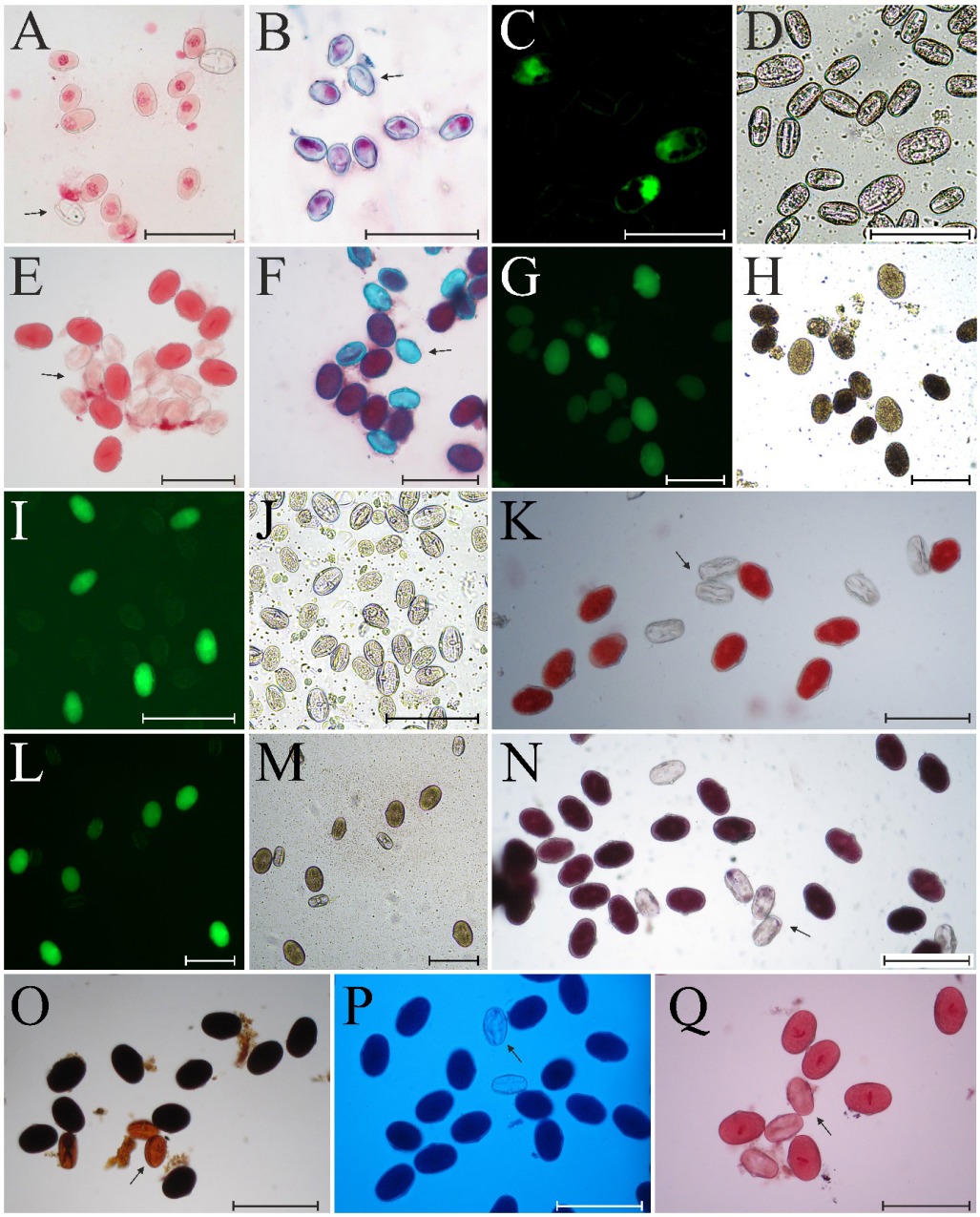

Figure 6. *Vicia faba* microspores (**A**–**D**,**I**,**J**) and pollen grains (**E**–**H**,**K**–**Q**) subjected to different staining methods: (**A**,**E**)—acetocarmine; (**B**,**F**)—Alexander's dye; (**C**,**D**,**G**,**H**)—Calcein method: (**C**,**G**)—the view in fluorescence, (**D**,**H**)—the same field of view in bright field microscopy; (**I**,**J**,**L**,**M**)—FDA method: (**I**,**L**)—the view in fluorescence, (**J**,**M**)—the same field of view in bright field microscopy; (**K**)—TTC method; (**N**)—MTT method; (**O**)—Lugol's iodine staining; (**P**)—aniline blue in lactophenol method; (**Q**)—aceto-orcein staining. Arrows indicate nonviable microspores or pollen grains. Bar = 100 μm.

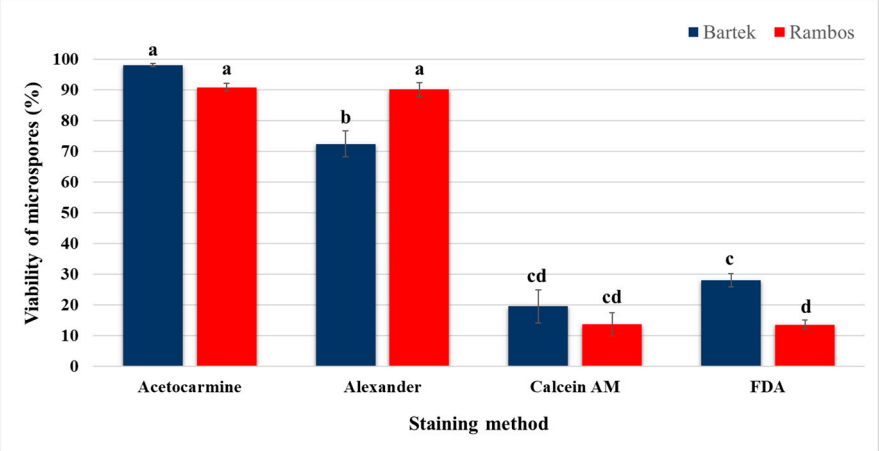

Figure 7. Viability of *Vicia faba* microspores determined with different staining methods depending on cultivar. Bars represent means ± SEM. Means denoted with the same letters are not significantly different (HSD, $p \leq 0.05$).

The average viability of the *V. faba* pollen grains, calculated as the mean from all the applied dyes and cultivars, was 80.55% (Table 1). The highest pollen viability (93–96%) was detected after application of the aniline blue in lactophenol and MTT dyes. Slightly fewer viable microspores (90.80%) were detected with the aceto-orcein method. Viability in the range of 84–86% was observed after application of acetocarmine, Lugol's iodine, and TCC. After application of Alexander's dye, 83% of the cells were detected as viable. Similarly, as was the case for the microspores, the lowest percentages of viable pollen grains were detected using Calcein AM and FDA (31.78% and 38.81%, respectively).

Figure 8 presents the pollen viability depending on the cultivar. Significant differences in pollen viability between 'Rambos' and 'Bartek' were observed after FDA staining (31.46% and 50.46%, respectively) and the aceto-orcein method (98.60% and 83.0%, respectively). After the application of other dyes, the differences in viability between the tested cultivars were slight (acetocarmine, Alexander's dye, calcein, Lugol's iodine, MTT, TCC) or the viability was similar (aniline blue in lactophenol).

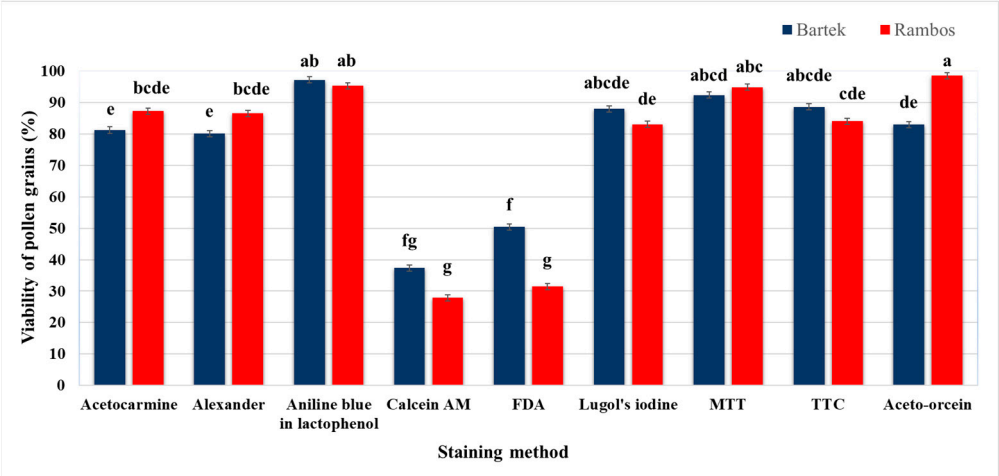

Figure 8. Viability of *Vicia faba* pollen grains determined using nine different staining methods depending on cultivar. Bars represent means ± SEM. Means denoted with the same letters are not significantly different (HSD, $p \leq 0.05$).

3.3.2. *Lupinus angustifolius*

The same set of stains was applied to *L. angustifolius* microspores and pollens. Analyses performed on microspores showed that six (acetocarmine, Alexander's dye, aniline blue in lactophenol, Calcein AM, FDA, and TTC) out of the nine tested allowed for discrimination between viable and nonviable cells (Table 2, Figure 9).

Table 2. Viability of *Lupinus angustifolius* microspores and pollen determined using different staining methods.

Staining Method	Viability (% ± SEM)	
	Microspores	Pollens
Acetocarmine	65.91 ± 1.94 ^{a}	85.18 ± 1.13 ^{ab}
Alexander's dye	54.83 ± 2.69 ^{b}	79.53 ± 1.71 ^{b}
Aniline blue in lactophenol	66.51 ± 2.77 ^{a}	92.93 ± 0.93 ^{a}
Calcein	9.71 ± 1.72 ^{c}	33.42 ± 2.56 ^{d}
FDA	5.73 ± 0.75 ^{c}	34.82 ± 2.15 ^{d}
Lugol's iodine	-	83.44 ± 1.62 ^{ab}
MTT	-	68.77 ± 2.91 ^{c}
TTC	64.92 ± 3.62 ^{a}	69.00 ± 3.86 ^{c}
Aceto-orcein	-	85.46 ± 1.71 ^{ab}
Total	55.61 ± 1.52	72.29 ± 1.03

Means in column with the same letters are not significantly different according to Tukey's HSD test ($p \leq 0.05$). The dyes marked with a dash did not allow for discrimination between viable and nonviable cells.

The analysis showed that acetocarmine stained viable microspores bright red, and in contrast to *V. faba* microspores, the nuclei were not visualized by this dye in *L. angustifolius* cells. Nonviable microspores were transparent (Figure 9A). Alexander's dye clearly discriminated between viable and nonviable microspores; in the former, the cytoplasm was stained dark purple with bright blue cell walls. In some microspores, the cytoplasm was partially stained, but when a larger part of the cytoplasmic content (≥3/4 of the cell volume) was stained, these cells were also treated as viable. Nonviable cells were bright blue (Figure 9B). Aniline blue in lactophenol stained the cytoplasm of *L. angustifolius* microspores dark blue; however, in some microspores the cytoplasm was shrunken and a transparent border between the cytoplasm and the cell wall was visible. Nonviable cells were transparent (Figure 9C). TTC stained *L. angustifolius* microspores very slightly. The cytoplasm of the viable microspores stained bright red, while nonviable microspores were transparent (Figure 9D). In this case, accurate distinction between viable and nonviable cells required careful microscopic observation, as the distinction was not obvious. The effects of the application of Calcein AM and FDA (fluorescent dyes) to *L. angustifolius* microspores were similar. Viable microspores emitted yellow-green fluorescence, while nonviable ones were not seen under UV light, because of their lack of emission of fluorescent light (Figure 9I–L). Similarly to *V. faba*, in some samples the fluorescent signals were weak. The remaining stains, i.e., Lugol's iodine, MTT, and aceto-orcein, were ineffective and did not allow for discrimination of viable and nonviable microspores of *L. angustifolius*.

The average viability of microspores, calculated as the mean from all the dyes that discriminated between viable and nonviable cells, was 55.61%; however, differences depending on the staining method were observed (Table 2). Similar high microspore viability was observed after staining with acetocarmine (65.91%), aniline blue in lactophenol (66.51%), and TCC (64.92%). Lower microspore viability (54.83%) was observed after application of Alexander's dye. The lowest indication of microspore viability was given by dyes detecting esterase activity; the percentages of viable microspores determined using Calcein AM and FDA were very low in contrast to other dyes employed in this research and were, respectively, 9.71% and 5.73%, which are nearly 6- to 12-fold lower compared with the other applied staining methods.

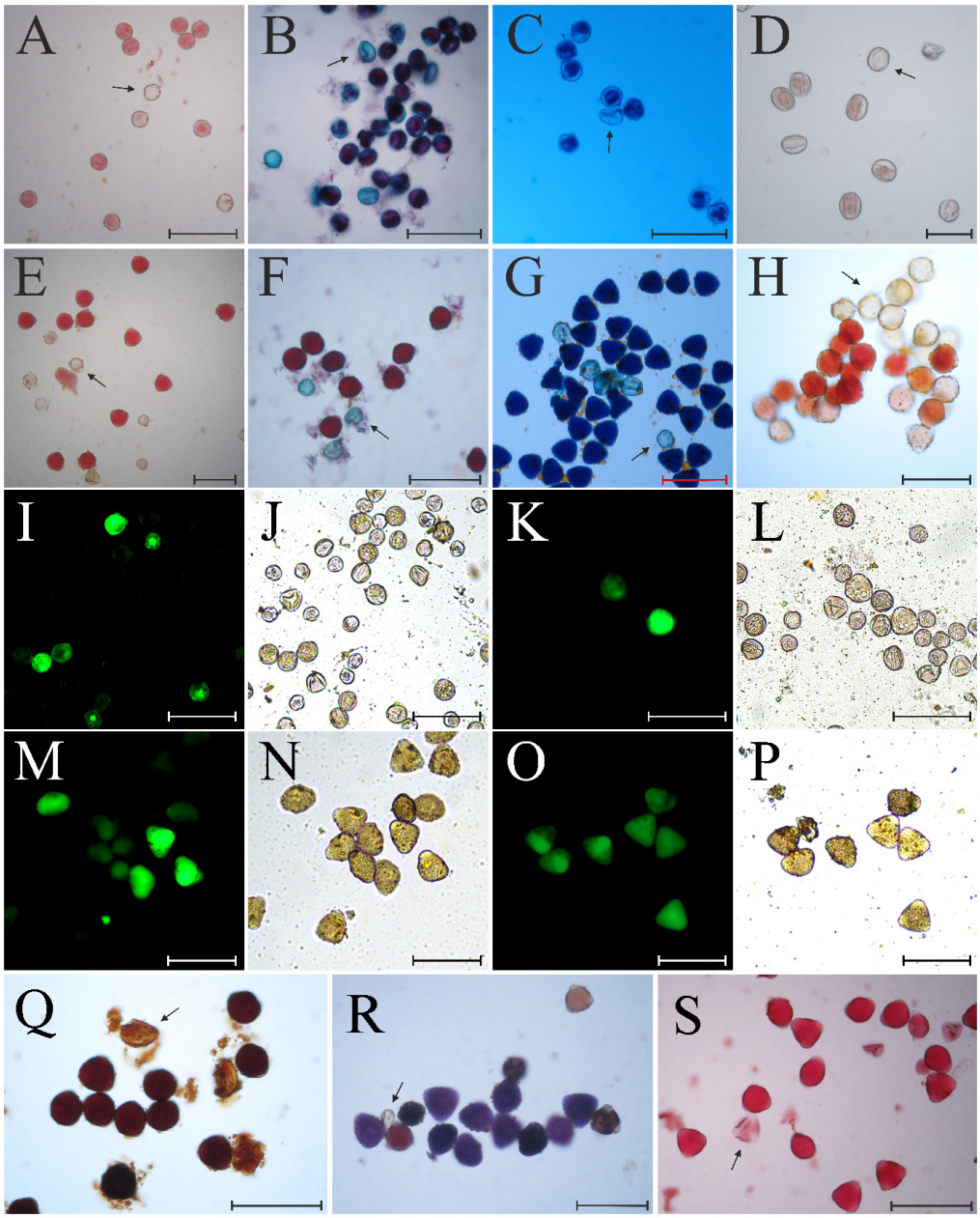

Figure 9. *Lupinus angustifolius* microspores (**A**–**D**,**I**–**L**) and pollen grains (**E**–**H**,**M**–**S**) subjected to different staining methods: (**A**,**E**)—acetocarmine staining; (**B**,**F**)—Alexander's staining; (**C**,**G**)—aniline blue in lactophenol method; (**D**,**H**)—TTC method; (**I**,**J**,**M**,**N**)—Calcein method: (**I**,**M**)—the view in fluorescence, (**J**,**N**)—the same field of view in bright field microscopy; (**K**,**L**,**O**,**P**)—FDA method: (**K**,**O**)—the view in fluorescence, (**L**,**P**)—the same field of view in bright field microscopy; (**Q**)—Lugol's iodine staining; (**R**)—MTT method; (**S**)—aceto-orcein staining. Arrows indicate nonviable microspores or pollen grains. Bar = 100 µm.

The interaction between cultivar and staining method on microspore viability was observed in *L. angustifolius* (Figure 10). A higher microspore viability for 'Regent' in comparison with 'Karo' was detected after application of Alexander's dye (65.54% and 43.65%, respectively) and aniline blue in lactophenol (79.90% and 53.40%, respectively). Contrast observations were made after application of acetocarmine (75.70% for 'Karo' and 56.10% for 'Regent') and TCC (79% for 'Karo' and 19.80% for 'Regent'). Similar to *V. faba*, the lowest percentages of viable microspores were detected using Calcein AM and FDA in both cultivars and they ranged from 5% to 12.3%, which was significantly different than the percentages of viable microspores determined with other methods.

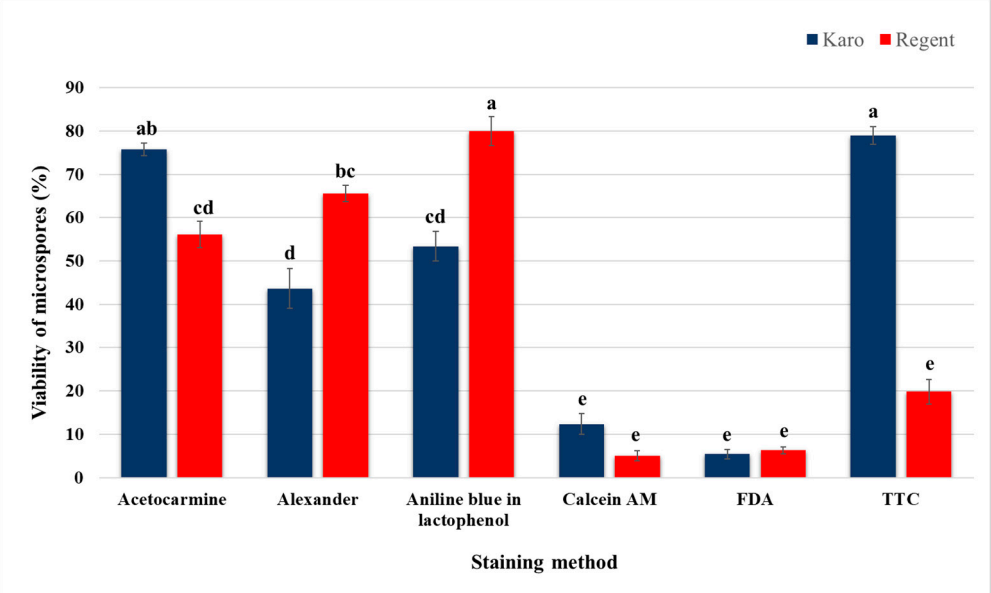

Figure 10. Viability of *Lupinus angustifolius* microspores determined using different staining methods depending on cultivar. Bars represent means ± SEM. Means denoted with the same letters are not significantly different ($p \leq 0.05$).

The analyses of the stainability of pollens of *L. angustifolius* showed that all tested dyes discriminate between viable and nonviable pollens (Figure 9). Acetocarmine stained mature pollen clearly and viable pollen turned red, but contrary to *V. faba* pollen, the nucleus was not visualized. Nonviable grains were transparent (Figure 9E). Alexander's dye stained the mature pollen of *L. angustifolius* differently than the microspores, as all of the cytoplasm was stained equally purple-red, in contrast to the microspores, which were stained dark purple. In nonviable cells, the cytoplasm was absent and the cell walls were stained blue (Figure 9F). Aniline blue in lactophenol staining allowed us to clearly differentiate between viable and nonviable pollen grains. In contrast to what was observed in microspores, the cytoplasm of mature pollen grains stained equally dark blue, and cytoplasm shrinkage or a transparent border between the cytoplasm and the cell wall were not observed. Nonviable cells were transparent or bright blue (Figure 9G). TTC also stained the mature pollen very clearly, and in general the viable cells turned red. However, some portions of *L. angustifolius* pollen stained darker/brighter than the others. The observed variation in coloration (from dark orange to dark red) of the cells suggests differentiated dehydrogenase activity, and such cells were all considered as viable. Pollens that were transparent were classified as nonviable (Figure 9H). Cells stained with Calcein AM and FDA under fluorescent microscopy emitted yellow-green fluorescence if viable, and did not emit fluorescence if nonviable (Figure 9M–P). After application of Calcein AM and FDA, the fluorescent signals in some cells were rather weak (Figure 9O). Lugol's iodine stained viable pollen grains of *L. angustifolius* the same as it did the *V. faba* pollens. Viable cells were dark brown and nonviable cells were bright brown or dark yellow. The shape of the nonviable pollen grains was also visually different from that of the viable ones. Viable cells were slightly triangular or rounded, contrary to the elongated and slightly flattened nonviable cells (Figure 9Q). After being stained with MTT and TTC, mature *L. angustifolius* pollen turned dark pink to dark purple if dehydrogenase enzymes were present in its cells, which proved their viability. Transparent cells were nonviable (Figure 9R). Aceto-orcein stained the cytoplasmic content of pollen grains of *L. angustifolius* dark pink, similarly to the *V. faba* pollens. However, unlike in *V. faba*, the cell nucleus was not visualized. Transparent or pale pink grains were considered as nonviable (Figure 9S).

The average pollen viability, calculated as the mean from all the dyes in *L. angustifolius*, was 72.29% (Table 2). The highest pollen viability (92.93%) was observed after staining

with aniline blue in lactophenol. This was followed by the viability percentages after application of acetocarmine (85.18%), Lugol's iodine (83.44%), and aceto-orcein (85.46%). Viability in the range 68–69% was observed after application of MTT and TCC. The lowest pollen viability was observed after staining with Calcein AM and FDA (33.42% and 34.82%, respectively).

The interaction between cultivar and staining method on pollen viability in *L. angustifolius* was also observed (Figure 11). After application of acetocarmine, Alexander's dye, aniline blue in lactophenol, Lugol's iodine, and aceto-orcein, there were no differences in pollen viability between 'Karo' and 'Regent' and viability ranged from 77.05% to 93.60%. The highest difference between cultivars in the rate of viable pollen grains was observed after application of stains detecting esterase activity. After MTT staining, a 52.21 percent point (37.21% in 'Karo' and 89.38% in 'Regent') difference in pollen viability between tested cultivars was observed, and after TTC staining, a 24 percent point (54.93% in 'Karo' and 78.97% in 'Regent') difference in pollen viability between tested cultivars was observed. The lowest viability (26.27–42.91%) was observed after application of fluorescent dyes (Calcein and FDA), and the results were similar for both cultivars.

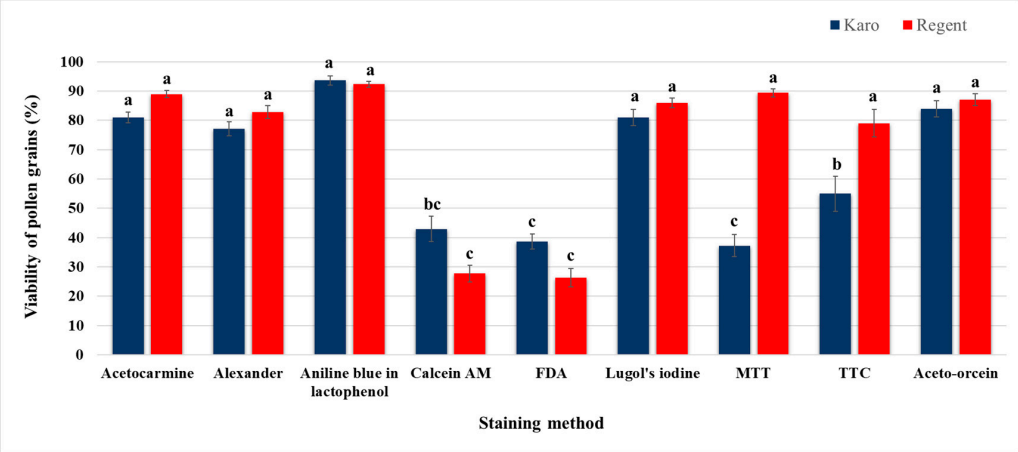

Figure 11. Viability of *Lupinus angustifolius* pollen grains determined using different staining methods depending on cultivar. Bars represent means ± SEM. Means denoted with the same letters are not significantly different ($p \leq 0.05$).

3.4. In Vitro Pollen Germination

During the analysis of in vitro pollen germination in *V. faba* and *L. angustifolius*, the following types of pollens were observed: germinated grains with fully developed typical pollen tubes (Figure 12A,D), germinated grains with deformed pollen tubes (thick or twisted) (Figure 12B,E), bursting pollen grains with irregular masses of cytoplasm protruding from the cells, and non-germinated pollens (Figure 12C,F). In this study, all grains with pollen tubes (typical and deformed) were counted as germinated, while bursting grains were excluded from the calculations of pollen germinability.

Analysis of pollen germination of both tested species showed a significant effect of the germination medium (Table 3). In *V. faba*, the highest germination rate (61.27%) was observed on the BK medium. Lower (43.30%) germination was observed on the G medium. In this species, only 11–17% of pollens germinated on the simplest media containing only sucrose. In *L. angustifolius*, the highest germination (70–74%) was observed on the medium supplemented with 10% sucrose and the G medium. Slightly lower germination (68.03%) was observed when pollen was applied onto the BK medium. The lowest germination (59.23%) was observed on the medium with 5% sucrose.

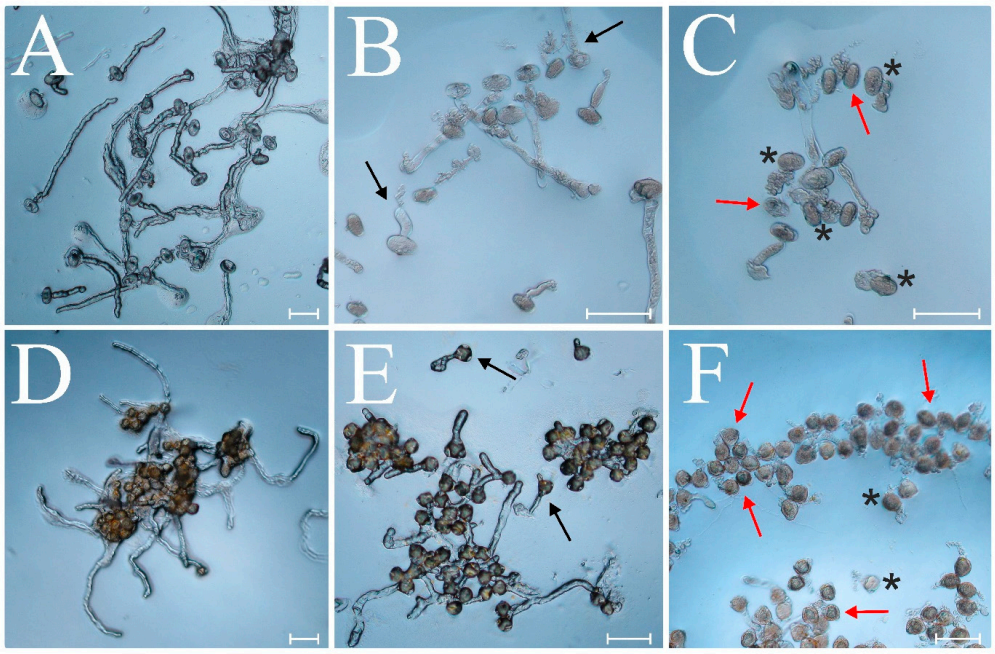

Figure 12. Phase contrast microphotography of *Vicia faba* (**A**–**C**) and *Lupinus angustifolius* (**D**–**F**) after in vitro pollen germination: (**A**,**D**)—germinated pollen grains with typical pollen tubes; (**B**,**E**)—pollen grains with deformed pollen tubes (indicated by black arrows); (**C**,**F**)—non-germinated pollen grains (indicated by red arrows). Asterisks indicate bursting of pollen grains. Bar = 100 µm.

Table 3. Viability of *Vicia faba* and *Lupinus angustifolius* pollens determined via in vitro pollen germination test.

Germination Media	Pollen Grain Germination (% ± SEM)	
	V. faba	***L. angustifolius***
Sucrose 5%	16.90 ± 2.04 ^{c}	59.23 ± 3.69 ^{b}
Sucrose 10%	10.84 ± 2.13 ^{c}	74.22 ± 2.76 ^{a}
G medium	43.30 ± 2.09 ^{b}	70.50 ± 2.38 ^{a}
BK medium	61.27 ± 2.23 ^{a}	68.03 ± 2.49 ^{ab}
Total	35.93 ± 1.88	67.99 ± 1.47

Means in column with the same letters are not significantly different according to Tukey's HSD test ($p \leq 0.05$).

In *V. faba*, differences in pollen germinability between the tested cultivars were observed (Figure 13). For each germinating medium, a higher percentage of germinated pollen grains was observed in 'Rambos' compared with 'Bartek'; however, statistically significant differences between the two cultivars occurred in two cases: on the medium containing 10% sucrose, where the pollen germinability of 'Bartek' was 5.80% and that of 'Rambos' was 21%, and on the BK medium, for which germinability was highest for both cultivars (53.30% in 'Bartek' and 69.20% in 'Rambos'). On the remaining media, the difference was slight.

In *L. angustifolius*, significant differences in pollen germination were observed only on the medium containing 5% sucrose (Figure 14). The pollen grain germinability was 49.50% in 'Regent' (which was the lowest result of germination of the *L. angustifolius* pollen grains) and 69% in 'Karo'. In other combinations (of cultivars and germination media), the percentages of germinated pollen grains were similar and ranged from 65.30% to 75.30%.

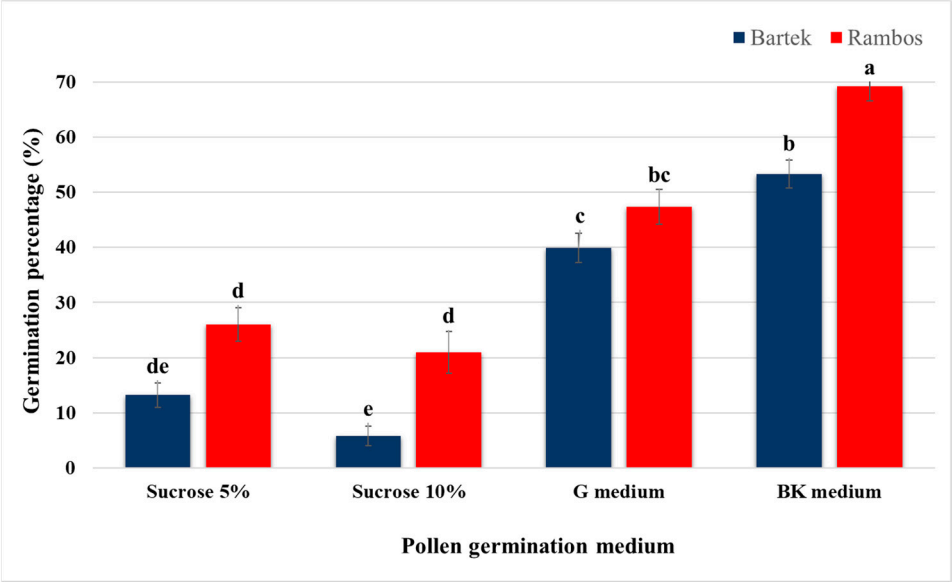

Figure 13. Viability of *Vicia faba* pollen grains determined via in vitro pollen germination test depending on the genotype. Bars represent means ± SEM. Means denoted with the same letters are not significantly different ($p \leq 0.05$).

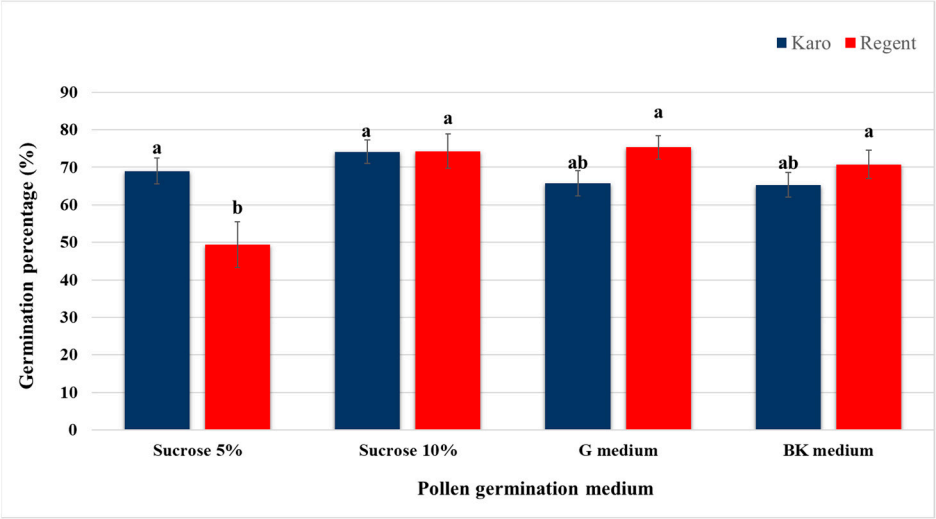

Figure 14. Viability of *Lupinus angustifolius* pollen grains determined via pollen germination test depending on the genotype. Bars represent means ± SEM. Means denoted with the same letters are not significantly different ($p \leq 0.05$).

4. Discussion

Pollen development begins in the locules of young anthers and consists of two major phases—microsporogenesis and microgametogenesis. In brief, microsporogenesis in plants is preceded by the formation of archesporial cells (ACs). PMCs are formed in the anther locules following the division of ACs located in the subepidermal position [39]. Further, meiotic division produces four haploid microspores (tetrads) enclosed within the callosic cell wall. Later, callose is degraded by the enzyme callase secreted by tapetum, which leads to the formation of individual microspores, which indicates microgametogenesis. Microspore development proceeds through a progressive cycle of vacuole biogenesis which involves fusion and fission events. Enlargement of vacuoles is associated with polarization of the microspore nucleus against the cell wall. Polarization provides a signal for asymmetric division (pollen mitosis I) that results in the formation of vegetative and

generative cells. The generative cell completes mitosis (pollen mitosis II) to form two sperm cells [40].

Compared with other members of the Fabaceae family, i.e., *Glycine* sp. [41], *Pisum* sp. [42–44], *Lens* sp. [42], or *Medicago* sp. [45], relatively little information is available about microsporogenesis and microgametogenesis in *Vicia* sp. and *Lupinus* sp. Mitchell [46] was the first to analyze macro- and microsporogenesis in *V. faba*. He observed that microspore development was initiated before meiosis in the megasporocyte and the microsporocyte meiosis proceeded through the normal meiotic process and ended with the formation of tetrads. At the stage of initiation of microsporocyte meiosis, the anther walls consisted of four undifferentiated layers, but as the cells progressed through zygotene and pachytene, tapetal cells became more distinct. A later study in *V. faba* revealed that during microsporogenesis, cytomixis (transmigration of chromatin between neighboring cells) might occur [47]. Cytomixis results in development of micronuclei or micropollens. The gametes with deficient chromosome numbers might be eliminated or produce aborted pollen, and gametes with different numbers of chromosomes may result in the formation of aneuploid or large-sized pollens [48]. Spontaneous cytomixis has also been observed in other legumes such as *M. sativa*, *P. vulgaris*, and *Lotus* sp. [44,49,50]. There is no comprehensive study on the microgametogenesis in *V. faba*. Within the species *Lupinus*, microgametogenesis was analyzed with a special focus on anther dehiscence in L. luteus [51]. In *L. elegans* and *L. mutabilis*, only microgametogenesis has been analyzed [52]. To the best of our knowledge, there are no studies on pollen development in *L. angustifolius*; therefore, we performed an analysis of the anatomy of the anthers at different stages of development in both *V. faba* and *L. angustifolius* and validated those findings with DAPI staining.

Our study showed that in *V. faba*, microgametogenesis initiation exhibited similar patterns in both genotypes. In 4 mm buds of both cultivars, mainly tetrads were found. A significant difference was observed in buds of a size of 5 mm, where in 'Bartek', tetrads still predominated (97.44%), whereas in the 'Rambos' buds, they occurred in the minority (41.76%) compared with uninucleate microspores. This indicates variations in the timing of microsporogenesis initiation among both cultivars of *V. faba*. On the other hand, in both cultivars of *L. angustifolius*, microgametogenesis followed a similar course. Uninucleate microspores were found in flower buds ranging from 4 to 7 mm, and occasionally in 8 mm buds. As an almost exclusive developmental stage, they occurred in flower buds of both cultivars at lengths of 4–5 mm. The range of their occurrence was also broader compared with that of *V. faba*, as they were found in flower buds of four and occasionally five different lengths, whereas in *V. faba*, they were found as a significant percentage in buds of only two or three lengths. Moreover, our study showed that both tested species formed tetraedric tetrads, and the released microspores were an isodiametric, circular shape. Differences were observed among pollens, as *V. faba* pollens were elliptic, and *L. angustifolius* pollens were circular but when fully hydrated were triangular. Moreover, both species produce bicellular pollen, as we did not observe tricellular pollens in any of the preparations made from flowers in full bloom. This implies that in both species the second pollen mitosis (pollen mitosis II) occurs within the growing pollen tube. Although the majority of flowering plants produce bicellular pollen, many important food crop plants such as rice, wheat, and maize produce short-lived, tricellular pollen grains [40].

The method of embedding tissue in synthetic resin which was performed here enabled effective analysis of the main stages of microsporogenesis and microgametogenesis, including anther development, in both species. According to our results, the walls of the anthers of *V. faba* and *L. angustifolius* consist of four layers: epidermal, endothecium, middle, and tapetal. At the PMC stage, all four layers were clearly distinguishable and the cells of the epidermis, endothecium, and middle layer were similar in size. The main observable difference was the presence of a nutritive tissue, the tapetum, which lined the inner walls of the anthers. The tapetum's primary function is to secrete nutrients and provide optimal conditions for the development of PMCs and microspores. After fulfilling their role, tapetal cells undergo degeneration through programmed cell death (PCD), and the anther walls consist of only the epidermis, endothecium, and middle layer [53,54]. In both *V. faba* and *L.*

angustifolius, the tapetum became distinct in the anthers containing PMCs. At this stage, the tapetal cells were larger compared with the cells or remaining layers of the anther walls. Moreover, these cells contained large nuclei. The increased size of the tapetal cells and nuclei in the analyzed species might be a result of endomitosis without cytokinesis and endoreduplication resulting in polyteny, which was already observed in the tapetal cells of other legumes [55,56]. At the tetrad stage, the tapetal cells in *V. faba* anthers were clearly seen as a distinct layer of cells, enlarged in size and possessing nuclei that were strongly stainable in toluidine blue. In *L. angustifolius* anthers, the tapetum stained deep blue and neither single cells nor the nuclei could be distinguished at this stage. Another difference was associated with the presence of tapetum and its morphology in the anthers containing uninucleate microspores. In *V. faba*, the tapetum was still clearly distinguished from the remaining anther layers, and its cells were large with centrally located, distinct cell nuclei. In this species, the tapetum disintegrated after uninucleate microspores went through mitosis, which is in agreement with the observations of Mitchell [46]. In *L. angustifolius* anthers, being at a similar stage of development, the tapetum was already degraded and appeared as a hazy, shapeless layer with a disorganized structure, located just below the middle layer of the anther wall. In the anthers containing binucleate pollen grains, the tapetum in both species was already degraded. These differences indicate a faster initiation of degradation of the tapetum in *L. angustifolius* compared with *V. faba*, suggesting a species-specific progression of this process. According to our observations, both *V. faba* and *L. angustifolius* generate secretory types of tapetum.

Another interesting feature concerned endothecium—a tissue that plays a crucial role in anther dehiscence and the release of pollen grains [57]. Lignification of endothecium walls is accompanied by the disappearance of the middle layer and tapetal cells as well as the formation of characteristic thickening [58], which was clearly observable in our study in both tested species. The endothecium cells were substantially larger than the epidermal cells. In the cross-section, the walls of the endothecium exhibited characteristic thickening corresponding to the strengthening ledges visible in their longitudinal sections.

According to many researchers' reports, the most reliable criterion of pollen viability assessment is the ability of pollen to fertilize and then produce a certain number of seeds by plant [59–61]. However, there are many factors affecting fertilization and seed production, i.e., genetics (self-incompatibility, control of seed development and dormancy, genetic load, and embryo abortion), environmental factors (growth conditions, nutrients, photoperiod, and humidity), the physiological status of the parental plants, hormonal regulation of flowering and seed development, etc. [62,63]. Thus, the lack of seed formation cannot be fully explained by the nonviability of the pollen. The in vitro pollen germination method is based on the simulation of the essential environment for the growth of pollen tubes under laboratory conditions, and therefore reflects the real capacity of pollen to fertilize and thus its viability [60]. However, this method is not universal and requires proper conditions, which vary depending on species in such factors as medium composition, sugar concentration, temperature, and humidity [62,64,65]. Contrary to pollen germination tests, staining methods are able to present only the relative viability of pollen or microspores based on the detection of single cell compounds like cytoplasmic content, enzymes, or constituents of the plant cell wall, e.g., callose. Thus, the inference concerning cell viability with this method is based on the presence of a single cell compound that allows us to obtain only an estimated indication of cell viability.

In this study, nine different chemical staining methods for estimating the pollen and microspore viability of *V. faba* and *L. angustifolius* were employed. For *V. faba*, there were four applied staining methods that were suitable for both microspore and pollen grain viability estimation, whereas for *L. angustifolius* there were six of them (the same ones as previously mentioned, as well as aniline blue in lactophenol and TTC). Among the staining methods employed for estimating *V. faba* pollen grain viability, five of them (aniline blue in lactophenol, TTC, MTT, Lugol's staining, and aceto-orcein) were excluded for microspore

viability testing, whereas for *L. angustifolius* microspore viability estimation three of the methods used were recognized as unsuitable (MTT, Lugol's staining, and aceto-orcein).

Many researchers have successfully used fluorescent dyes, such as FDA or Calcein AM, to assess membrane integrity and esterase activity for determining the viability of mature pollen or microspores in various species, including *Cucumis sativus* [19], *Solanum lycopersicum* [66], *Mangifera indica* [67], *Vitis vinifera* [68], *Viola tricolor* [69], *Juglans regia* [70], *Annona cherimola*, and *Olea europaea* [71], as well as other species from the *Fabaceae* family, such as *Phaseolus acutifolium* [72], *Cicer arietinum* [73], and *Pisum sativum* [74]. The viability results obtained using FDA in the above-cited studies were relatively high and did not significantly differ from the results obtained using other methods, such as TTC, MTT, or in vitro pollen germination, and sometimes even exceeded those values, as observed for *V. tricolor* and *M. indica*. In our study, the use of FDA and Calcein AM for assessing the viability of microspores and pollens in both species yielded very low viability readings compared with other applied staining methods and with the in vitro pollen germination test. Particularly, when compared with the assessment of pollen germination, which is considered a more reliable and accurate method for pollen viability evaluation, the results obtained for fluorescent dyes were significantly underestimated. The reasons for this can be attributed to the morphological structure of the microspores and pollen grains in the investigated species, particularly the thickness of the exine and intine comprising the cell walls of these cells. This could affect the mobility of FDA and Calcein AM and consequently limit the ability of these dyes to penetrate the interior of the cell. Clarke and Kupicha [75] assessed the cell wall of *Vicia pollen* as relatively thick, measuring 1.5–1.75 µm in the polar region. On the other hand, Kahraman et al. [76] conducted a morphological analysis of pollen grains from 11 species belonging to the *Vicia* genus and indicated that the exine thickness ranged from 0.92 to 1.50 µm, while the intine thickness ranged from 0.69 to 1.15 µm. For comparison, the intine thickness of Pisum sativum pollen was reported to range from 0.222 to 0.414 µm [77]. Due to the uncertainties arising from the mentioned observations, further investigations and additional analyses are required to identify the causes of such circumstances. A comprehensive understanding of the ultrastructure of the cell walls of *V. faba* and *L. angustifolius* pollens and microspores may provide valuable insights and a probable explanation.

The analysis of pollen germination in vitro revealed different germination capacities among the studied species depending on the medium used. In *V. faba*, the highest pollen germination was achieved on the Brebaker and Kwack's [37] (BK) medium, while other tested media, particularly those containing only sucrose, significantly reduced the germination capacity. The BK medium has been successfully employed with other *Fabaceae* species such as *Cicer arietinum* [78], *Cajanus cajan* [79], *Pisum sativum* [80], *Humboldtia sanjappae* [81], and *Swainsona formosa* [82] and, as proven by our study, was also suitable for effective in vitro pollen germination for *V. faba*. In contrast, in *L. angustifolius* relatively high percentages of germinating pollen grains were observed on all tested culture media.

5. Conclusions

Up until now, there has been a lack of available literature concerning the processes of microsporogenesis and microgametogenesis in *V. faba* and *L. angustifolius*, or it has been limited in scope. The conducted research fills this gap and provides detailed analyses of how anthers and pollen develop in the studied species. The comprehensive analysis of microspore and pollen viability revealed that the issue of determining viability is particularly challenging for microspores but not for pollen, as all nine tested dyes proved to be applicable to pollens but only four were applicable to microspores. Dyes detecting esterase activity (FDA and Calcein AM) were problematic due to their significant underestimation of microspore and pollen viability results compared with other methods, including pollen germination. This highlights the species-specific nature of the issue and calls for the optimization and development of effective protocols for applying these dyes in the studied species. The comprehensive analysis performed in this study addressed the challenges

related to microspore and pollen viability assessment and opened possibilities for future developments and progress in understanding the reproductive biology of *V. faba* and *L. angustifolius* and improving their breeding programs through haploidization.

Author Contributions: Conceptualization, A.K.; methodology, A.K. and W.S.; software, W.S.; formal analysis, A.K. and W.S.; investigation, W.S. and A.K.; resources, W.S. and A.K.; data curation, W.S. and A.K.; writing—original draft preparation, W.S. and A.K.; writing—review and editing, W.S. and A.K.; visualization, W.S. and A.K.; supervision, A.K.; project administration, A.K. and R.G.; funding acquisition, A.K., R.G. and A.A. All authors have read and agreed to the published version of the manuscript.

Funding: This research was funded by the Polish Ministry of Agriculture and Rural Development (grant no. DHR.hn.802.13.2022 awarded to A.K. and grant no. KS.zb.802.8.2020 awarded to R.G.).

Institutional Review Board Statement: Not applicable.

Data Availability Statement: Not applicable.

Conflicts of Interest: The authors declare no conflict of interest.

References

1. FAOSTAT. Access Protocol. 2021. Available online: https://www.fao.org/faostat/en/#data/QCL/visualize (accessed on 4 September 2023).
2. Shavanov, M.V. The Role of Food Crops within the *Poaceae* and *Fabaceae* Families as Nutritional Plants. In *IOP Conference Series: Earth and Environmental Science*; IOP Publishing: Bristol, UK, 2021; Volume 624, p. 012111. [CrossRef]
3. Bangar, S.P.; Kajla, P. Introduction: Global Status and Production of Faba-Bean. In *Faba Bean: Chemistry, Properties and Functionality*; Springer International Publishing: Berlin/Heidelberg, Germany, 2022; pp. 1–15.
4. Smýkal, P.; Coyne, C.J.; Ambrose, M.J.; Maxted, N.; Schaefer, H.; Blair, M.W.; Berger, J.; Greene, S.L.; Nelson, M.N.; Besharat, N.; et al. Legume crops phylogeny and genetic diversity for science and breeding. *Crit. Rev. Plant Sci.* **2015**, *34*, 43–104. [CrossRef]
5. Farooq, M.; Gogoi, N.; Hussain, M.; Barthakur, S.; Paul, S.; Bharadwaj, N.; Hussein, M.; Migdadi, S.S.; Alghamdi, K.H.M. Siddique. Effects, tolerance mechanisms and management of salt stress in grain legumes. *Plant Physiol. Biochem.* **2017**, *118*, 199–217. [CrossRef] [PubMed]
6. Erdemoglu, N.; Ozkan, S.; Tosun, F. Alkaloid profile and antimicrobial activity of *Lupinus angustifolius* L. alkaloid extract. *Phytochem. Rev.* **2007**, *6*, 197–201. [CrossRef]
7. Kohajdová, Z.; Karovičová, J.; Schmidt, Š. Lupin composition and possible use in bakery-a review. *Czech J. Food Sci.* **2011**, *29*, 203–211. [CrossRef]
8. Di Cenzo, G.C.; Tesi, M.; Pfau, M.A.; Fondi, M. Genome-scale metabolic reconstruction of the symbiosis between a leguminous plant and a nitrogen-fixing bacterium. *Nat. Commun.* **2020**, *11*, 2574. [CrossRef]
9. Lassoued, R.; Macall, D.M.; Smyth, S.J.; Phillips, P.W.; Hesseln, H. How should we regulate products of new breeding techniques? Opinion of surveyed experts in plant biotechnology. *Biotechnol. Rep.* **2020**, *26*, e00460. [CrossRef] [PubMed]
10. Żur, I.; Adamus, A.; Cegielska-Taras, T.; Cichorz, S.; Dubas, E.; Gajecka, M.; Juzoń-Sikora, K.; Kiełkowska, A.; Malicka, M.; Oleszczuk, S.; et al. Doubled Haploids: Contributions of Poland's Academies in recognizing the mechanism of gametophyte cell reprogramming and their utilization in breeding of agricultural and vegetable species. *Acta Soc. Bot. Pol.* **2022**, *91*, 9128. [CrossRef]
11. Kiełkowska, A.; Kiszczak, W. History and current status of haploidization in carrot (*Daucus carota* L.). *Agronomy* **2023**, *13*, 676. [CrossRef]
12. Małuszyński, M.; Kasha, K.J.; Forster, B.P.; Szarejko, I. (Eds.) *Doubled Haploid Production in Crop Plants. A Manual*; Kluwer Academic Publishers: Dordrecht, The Netherlands, 2003; p. 428.
13. Germanà, M.A. Doubled haploid production in fruit crops. *Plant Cell Tiss. Organ. Cult.* **2006**, *86*, 131–146. [CrossRef]
14. Kiełkowska, A.; Adamus, A.; Barański, R. An improved protocol for carrot haploid and doubled haploid plant production using induced parthenogenesis and ovule excision in vitro. *Vitr. Cell Dev. Biol. Plant* **2014**, *50*, 376–383. [CrossRef]
15. Paratasilpin, T. Vegetative development of field bean pollen grain cultured in vitro. *J. Sci. Soc. Thai* **1978**, *4*, 139–145.
16. Skrzypek, E.; Czyczyło-Mysza, I.; Marcińska, I.; Wędzony, M. Prospects of androgenetic induction in *Lupinus* spp. *Plant Cell Tiss. Organ. Cult.* **2008**, *94*, 131–137. [CrossRef]
17. Kozak, K.; Galek, R.; Waheed, M.T.; Sawicka-Sienkiewicz, E. Anther culture of *Lupinus angustifolius*: Callus formation and the development of multicellular and embryo-like structures. *Plant Growth Regul.* **2012**, *66*, 145–153. [CrossRef]
18. Shlahi, S.A.; Majeed, D.M.; Ismail, E.N. Effect of the developmental stage of microspores, growth regulator and medium type on callus indication from broad bean *Vicia faba* anthers culture. *Res. J. Biotechnol.* **2012**, *6*, 81–90. [CrossRef]
19. Vizintin, L.; Bohanec, B. In vitro manipulation of cucumber (*Cucumis sativus* L.) pollen and microspores: Isolation procedures, viability tests, germination, maturation. *Acta Biol. Cracov Ser. Bot.* **2004**, *46*, 177–183.

20. Impe, D.; Reitz, J.; Köpnick, C.; Rolletschek, H.; Börner, A.; Senula, A.; Nagel, M. Assessment of pollen viability for wheat. *Front. Sci.* **2020**, *10*, 1588. [CrossRef]
21. Beyhan, N.; Serdar, U. Assessment of pollen viability and germinability in some European chestnut genotypes (*Castanea sativa* L.). *Hortic. Sci.* **2008**, *35*, 171–178. [CrossRef]
22. Hauser, E.J.P.; Morrison, J.H. The cytochemical reduction of nitroblue tetrazolium as an index of pollen viability. *Am. J. Bot.* **1964**, *51*, 748–752. [CrossRef]
23. Stern, W.L.; Curry, K.J.; Pridgeon, A.M. Osmophores of *Stanhopea* (*Orchidaceae*). *Am. J. Bot.* **1987**, *74*, 1323–1331. [CrossRef]
24. Nassar, N.M.A.; Santos, E.D.; David, S.R.O. The transference of apomixis genes from *Manihot neusana* Nassar to cassava, M. eculenta Crantz. *Hereditas* **2000**, *132*, 167–170. [CrossRef]
25. Rodriguez-Riano, T.; Dafni, A. A new procedure to assess pollen viability. *Sex. Plant Reprod.* **2000**, *12*, 241–244. [CrossRef]
26. Norton, J.D. Testing of plum pollen viability with tetrazolium salts. *Proc. Am. Soc. Hort. Sci.* **1966**, *89*, 132–134.
27. Heslop-Harrison, J.; Heslop-Harrison, Y.; Shivanna, K.R. The evaluation of pollen quality and a further appraisal of the fluorochromatic (FCR) test procedure. *Theor. Appl. Genet.* **1984**, *67*, 367–375. [CrossRef] [PubMed]
28. Kiełkowska, A.; Dziurka, M. Changes in polyamine pattern mediates sex differentiation and unisexual flower development in monoecious cucumber (*Cucumis sativus* L.). *Physiol. Plant* **2021**, *171*, 48–65. [CrossRef] [PubMed]
29. Barrow, J.R. Comparisons among pollen viability measurement methods in cotton 1. *Crops Sci.* **1983**, *23*, 734–736. [CrossRef]
30. Rathod, V.; Behera, T.K.; Munshi, A.D.; Durgesh, K.; Jat, G.S.; Krishnan, B.G.; Sharma, N. Pollen viability and in vitro pollen germination studies in *Momordica* species and their intra and interspecific hybrids. *Int. J. Chem. Stud.* **2018**, *6*, 32–40.
31. Rossel, P.; Herrero, M.; Galan Sauco, V. Pollen germination of cherimoya (*Annona cherimola* Mill). In vivo characterization and optimization of in vitro germination. *Sci. Hortic.* **1999**, *81*, 251–265. [CrossRef]
32. Adaniya, S. Optimal pollination environment of tetraploid ginger (*Zingiber officinale* Roscoe) evaluated by in vitro pollen germination and pollen tube growth in styles. *Sci. Hortic.* **2001**, *90*, 219–226. [CrossRef]
33. Alexander, M.P. Differential staining of aborted and nonaborted pollen. *Biotech. Histochem.* **1969**, *44*, 117–122. [CrossRef]
34. Gamborg, O.L.; Miller, R.A.; Ojima, K. Nutrient requirements of suspension cultures of soybean root cells. *Exp. Cell Res.* **1968**, *50*, 151–158. [CrossRef]
35. Johnson, S.; Nguyen, V.; Coder, D. Assessment of cell viability. *Curr. Protoc. Cytom.* **2013**, *64*, 9.2.1–9.2.26. [CrossRef] [PubMed]
36. Steward, N.; Martin, R.; Engasser, J.; Goergen, J.L. A new methodology for plant cell viability assessment using intracellular esterase activity. *Plant Cell Rep.* **1999**, *19*, 171–176. [CrossRef]
37. Brewbaker, J.L.; Kwack, B.H. The Essential role of calcium ion in pollen germination and pollen tube growth. *Am. J. Bot.* **1963**, *50*, 859. [CrossRef]
38. Gaaliche, B.; Majdoub, A.; Trad, M.; Mars, M. Assessment of pollen viability, germination, and tube growth in eight Tunisian caprifig (*Ficus carica* L.) cultivars. *ISRN Agron.* **2013**, *13*, 1–4. [CrossRef]
39. Feng, X.; Zilberman, D.; Dickinson, H. A conversation across generations: Soma-germ cell crosstalk in plants. *Dev. Cell* **2013**, *24*, 215–225. [CrossRef] [PubMed]
40. Honys, D.; Renák, D.; Twell, D. Male Gametophyte Development and Function. In *Floriculture, Ornamental and Plant Biotechnology: Advances and Topical Issues*; Silva, J.T., Ed.; Global Science Books: London, UK, 2006; Volume 1, pp. 76–87.
41. Albertsen, M.C.; Palmer, R.G. A comparative light—And electron-microscopic study of microsporogenesis in male sterile (ms1) and male fertile soybeans (*Glycine max* (L.) merr.). *Am. J. Bot.* **1979**, *66*, 253–265. [CrossRef]
42. Biddle, J.A. Anther and pollen development in garden pea and cultivated lentil. *Can. J. Bot.* **1979**, *57*, 1883–1900. [CrossRef]
43. Myers, J.R.; Gritton, E.T.; Struckmeyer, B.E. Genetic male sterility in the pea (*Pisum sativum* L.). *Euphytica* **1992**, *63*, 245–256. [CrossRef]
44. Kumar, G.; Chaudhary, N. Induced cytomictic variations and syncyte formation during microsporogenesis in *Phaseolus vulgaris* L. *Cytol. Genet.* **2016**, *50*, 121–127. [CrossRef]
45. Tavoletti, S.; Mariani, A.; Veronesi, F. Cytological analysis of macro- and microsporogenesis of a diploid alfalfa clone producing male and female 2n gametes. *Crops Sci.* **1991**, *31*, 1258–1263. [CrossRef]
46. Mitchell, J.P. Megasporogenesis and microsporogenesis in *Vicia faba*. *Can. J. Bot.* **1975**, *53*, 2804–2812. [CrossRef]
47. Haroun, S.A.; Al Shehri, A.M.; Al Wadie, H.M. Cytomixis in the microsporogenesis of *Vicia faba* L. (*Fabaceae*). *Cytologia* **2004**, *69*, 7–11. [CrossRef]
48. Mursalimov, S.; Deineko, E. Cytomixis in plants: Facts and doubts. *Protoplasma* **2018**, *255*, 719–731. [CrossRef] [PubMed]
49. Gottschalk, W. Chromosome and nucleus migration during microsporogenesis of *Pisum sativum*. *Nucleus* **1970**, *13*, 1–9.
50. Bellucci, M.; Roscini, C.; Mariani, A. Cytomixis in pollen mother cells of *Medicago sativa* L. *J. Hered.* **2003**, *94*, 512–516. [CrossRef] [PubMed]
51. Marciniak, K.; Przedniczek, K. Anther dehiscence is regulated by gibberellic acid in yellow lupine (*Lupinus luteus* L.). *BMC Plant Biol.* **2021**, *21*, 314. [CrossRef] [PubMed]
52. Wojciechowska, W. The development rhythm of the flower bud in some *Papilionaceae* species. Gametogenesis in *L. elegans* (H.B.K.) nad *Lupinus mutabilis* (Sweet.) in reference to flower bud development. *Acta Soc. Bot. Pol.* **1976**, *45*, 251–262. [CrossRef]
53. Papini, A.; Mosti, S.; Brighigna, L. Programmed-cell-death events during tapetum development of angiosperms. *Protoplasma* **1999**, *207*, 213–221. [CrossRef]
54. Furness, C.A.; Rudall, P.J. The tapetum in basal angiosperms: Early diversity. *Int. J. Plant Sci.* **2001**, *162*, 375–392. [CrossRef]

55. Guerra, M.; Carvalheira, G. Occurrence of polytene chromosomes in the anther tapetum of *Vigna unguiculata* L. (Walp.). *J. Hered.* **1994**, *85*, 43–46.
56. Carvalheira, G.; Guerra, M. The polytene chromosomes of anther tapetum of some *Phaseolus* species. *Cytologia* **1994**, *59*, 211–217. [CrossRef]
57. Cecchetti, V.; Altamura, M.M.; Brunetti, P.; Petrocelli, V.; Falasca, G.; Ljung, K.; Costantino, P.; Cardarelli, M. Auxin controls *Arabidopsis* anther dehiscence by regulating endothecium lignification and jasmonic acid biosynthesis. *Plant J.* **2013**, *74*, 411–422. [CrossRef] [PubMed]
58. Kostryco, M.; Chwil, M. Structure of Anther Epidermis and Endothecium, Production of Pollen, and Content of Selected Nutrients in Pollen Grains from Six *Rubus idaeus* L. Cultivars. *Agronomy* **2021**, *11*, 1723. [CrossRef]
59. Grigg, F.D.; Smith, P.R.; Stenersen, M.A.; Murray, B.G. Variable pollen fertility and abnormal chromosome behavior in the pepino (*Solanum muricatum* Ait., *Solanaceae*). *Sci. Hortic.* **1988**, *35*, 259–268. [CrossRef]
60. Shivanna, K.R.; Linskens, H.F.; Cresti, M. Pollen viability and pollen vigor. *Theor. Appl. Genet.* **1991**, *81*, 38–42. [CrossRef] [PubMed]
61. Gibernau, M.; Macquart, D.; Diaz, A.; House, D.; Fern-Barrow, P.; Dorset, B. Pollen viability and longevity in two species of *Arum*. *Aroideana* **2003**, *26*, 58–62.
62. Dafni, A.; Firmage, D. Pollen viability and longevity: Practical, ecological and evolutionary implications. *Pollen Pollinat.* **2000**, 113–132. [CrossRef]
63. Bareke, T. Biology of seed development and germination physiology. *Adv. Plants Agric. Res.* **2018**, *8*, 336–346. [CrossRef]
64. Stanley, R.G.; Linskens, H.F. *Pollen: Biology, Biochemistry and Management*; Springer: New York, NY, USA, 1974. [CrossRef]
65. Patel, R.G.; Mankad, A.U. In vitro pollen germination—A review. *Int. J. Sci. Res.* **2014**, *3*, 304–307.
66. Seguí-Simarro, J.M.; Nuez, F. Embryogenesis induction, callogenesis, and plant regeneration by in vitro culture of tomato isolated microspores and whole anthers. *J. Exp. Bot.* **2007**, *58*, 1119–1132. [CrossRef]
67. Dutta, S.K.; Srivastav, M.; Chaudhary, R.; Lal, K.; Patil, P.; Singh, S.K.; Singh, A.K. Low temperature storage of mango (*Mangifera indica* L.) pollen. *Sci. Hortic.* **2013**, *161*, 193–197. [CrossRef]
68. Kelen, M.; Demirtas, I. Pollen viability, germination capability and pollen production of some grape varieties (*Vitis vinifera* L.). *Acta Physiol. Plant* **2003**, *25*, 229–233. [CrossRef]
69. Słomka, A.; Kawalec, P.; Kellner, K.; Jedrzejczyk-Korycińska, M.; Rostański, A.; Kuta, E. Was reduced pollen viability in *Viola tricolor* L. the result of heavy metal pollution or rather the tests applied? *Acta Biol. Crac. Ser. Bot.* **2010**, *52*, 123–127. [CrossRef]
70. Ozcan, A.; Sutyemez, M.; Bukucu, S.B.; Ergun, M. Pollen viability and germinability of walnut: A comparison between storage at cold and room temperatures. *Fresenius Environ. Bull.* **2019**, *28*, 111–115.
71. Pinillos, V.; Cuevas, J. Standardization of the flourochromatic reaction test to assess pollen viability. *Biotech. Histochem.* **2008**, *83*, 15–21. [CrossRef] [PubMed]
72. Lord, E.M.; Kohorn, L.U. Gynoecial development, pollination, and the path of pollen tube growth in the tepary bean, *Phaseolus acutifolius*. *Am. J. Bot.* **1986**, *73*, 70–78. [CrossRef]
73. Fang, X.; Turner, N.C.; Yan, G.; Li, F.; Siddique, K.H.M. Flower numbers, pod production, pollen viability, and pistil function are reduced and flower and pod abortion increased in chickpea (*Cicer arietinum* L.) under terminal drought. *J. Exp. Bot.* **2010**, *61*, 335–345. [CrossRef] [PubMed]
74. Jiang, Y.; Lahlali, R.; Karunakaran, C.; Warkentin, T.D.; Davis, A.R.; Bueckert, R.A. Pollen, ovules, and pollination in pea: Success, failure, and resilience in heat. *Plant Cell Environ.* **2019**, *42*, 354–372. [CrossRef]
75. Clarke, G.C.S.; Kupicha, F.K. The relationships of the genus *Cicer*, L. (*Leguminosae*): The evidence from pollen morphology. *Bot. J. Linn. Soc.* **1976**, *72*, 35–44. [CrossRef]
76. Kahraman, A.; Binzat, O.K.; Doğan, M. Pollen morphology of some taxa of *Vicia*, L. subgenus *Vicia* (*Fabaceae*) from Turkey. *Plant Syst. Evol.* **2013**, *299*, 1749–1760. [CrossRef]
77. Jiang, Y.; Lahlali, R.; Karunakaran, C.; Kumar, S.; Davis, A.R.; Bueckert, R.A. Seed set, pollen morphology and pollen surface composition response to heat stress in field pea. *Plant Cell Environ.* **2015**, *38*, 2387–2397. [CrossRef] [PubMed]
78. Srinivasan, A.; Saxena, N.P.; Johansen, C. Cold tolerance during early reproductive growth of chickpea (*Cicer arietinum* L.): Genetic variation in gamete development and function. *Field Crops Res.* **1999**, *60*, 209–222. [CrossRef]
79. Jayaprakash, P.; Sarla, N. Development of an improved medium for germination of *Cajanus cajan* (L.) Millsp. pollen in vitro. *J. Exp. Bot.* **2001**, *52*, 851–855. [CrossRef] [PubMed]
80. Perveen, A. Pollen germination capacity, viability and Maintanence of *Pisum sativum* L. *papilionaceae*. *Middle East. J. Sci. Res.* **2007**, *2*, 79–81.
81. Jayalakshmi, M.; Sreekala, A.K.; Theresa, M. Floral biology of *Humboldtia sanjappae* Sasidh. & Sujanapal (*Fabaceae*). *J. Palynol.* **2016**, *52*, 1–13.
82. Zulkarnain, Z.; Eliyanti, E.; Swari, E.I. Pollen viability and stigma receptivity in *Swainsona formosa* (G. Don) J. Thompson (*Fabaceae*), an ornamental legume native to Australia. *Ornam. Hortic.* **2019**, *25*, 158–167. [CrossRef]